

Supporting Information

Electrochemical Instability of Highly Fluorinated Tetraphenyl Borates and the Syntheses of their Respective Biphenyls

Sebastian B. Beil, Sabine Möhle, Patrick Enders, and Siegfried R. Waldvogel

Contents

1. General Information.....	2
2. Experimental Setup	3
3. General Protocol for the Electrochemical Biphenyl Synthesis from Tetraphenylborates	4
4. Optimization of the Electrolysis Parameters.....	4
a) Electrochemical Synthesis of 3,3',5,5'-Tetrakis(trifluoromethyl)biphenyl (5) from Sodium Tetrakis(3,5-di(trifluoromethyl))phenyl)borate (Na-3)	4
b) Electrochemical Synthesis of Decafluorobiphenyl (4) from Lithium Tetrakis(pentafluorophenyl)borate (Li-2)	7
5. Characterization of Biphenyls.....	9
6. Synthesis of the Unsymmetric Tetraphenyl Borate 7 and Biphenyl 8.....	10
7. Cyclic Voltammetry Studies.....	12
a) Tetraphenylborates as Supporting Electrolyte.....	12
b) Tetraphenylborates as Substrates.....	16
8. NMR Spectra.....	31
9. References.....	38

1. General Information

All reagents were used in analytical grades and were obtained from commercial suppliers. Cyclohexane and ethyl acetate were of technical grade and distilled prior to use. Acetonitrile was of HPLC grade (Fisher Scientific) and dried over molecular sieve (3 Å). 1,1,1,3,3,3-Hexafluoroisopropanol (HFIP, 99%, Fluorochem) was dried over molecular sieve (3 Å), used HFIP was dried over P₄O₁₀ and redistilled (water and methanol impurities were identified by ¹H NMR spectroscopy, see NMR Spectra). Methanol was of reagent grade (Sigma Aldrich), dichloromethane and diethyl ether were of analysis grade (Fisher Scientific, Sigma Aldrich). Tetrabutylammonium tetraphenylborate (99%) was obtained from Sigma Aldrich, lithium tetrakis(pentafluorophenyl)borate etherate from Boulder Scientific Company and sodium tetrakis(3,5-bis(trifluoromethyl)phenyl)borate (97%) from Ark Pharm.

Column chromatography was performed on silica gel 60 M (0.040-0.063 mm, Macherey-Nagel GmbH&Co, Düren, Germany). A Sepacore® flash chromatography system (Büchi, Flawil, Switzerland) was used with flow rates of maximum 100 mL/min and maximum pressures of 10 bar. The flash chromatography system consists of a Büchi Control Unit C 620, an UV detector Büchi UV photometer C 635, a Büchi fraction collector C 660 and two Pump Modules C 605 for adjusting the solvent mixtures. As eluents, mixtures of cyclohexane and ethyl acetate were used. Silica gel 60 sheets on aluminum (F254, Merck, Darmstadt, Germany) were employed for thin layer chromatography.

Gas chromatography was performed on a Shimadzu GC-2010 and a GC-2025 (Shimadzu, Japan), respectively using a Zebron ZB-5MSi quartz capillary column (Phenomenex, USA; length: 30 m, inner diameter: 0.25 mm, film: 0.25 µm; carrier gas: hydrogen, injector temperature: 250 °C). The detector is a flame ionization detector (FID) with a temperature of 310 °C. GC-MS measurements were carried out with a Shimadzu GC-2010 (Shimadzu, Japan) using a Zebron ZB-5MSi quartz capillary column (Phenomenex, USA; length: 30 m, inner diameter: 0.25 mm, film: 0.25 µm, carrier gas: helium). The chromatograph was coupled to a mass spectrometer: Shimadzu GCMS-QP2010. The ion source (EI) has a temperature of 200 °C.

NMR spectroscopy: ¹H NMR, ¹³C NMR, ¹⁹F NMR and ¹¹B NMR were recorded at 25 °C on a Bruker Avance II 400 (400 MHz), Avance III HD 400 (400 MHz) and Avance III 600 (600 MHz) instrument (Bruker, Karlsruhe, Germany). Chemical shifts (δ) are reported in parts per million (ppm). Traces of non-deuterated solvents were used as internal standard for calibration. ¹⁹F shifts are indicated relative to C(³⁵Cl)₂(³⁷Cl)F. Calibration of the spectrometer prior to measurement was performed with α,α,α-trifluorotoluene in CDCl₃ (-63.9 ppm). For ¹¹B shifts were referred against BF₃*Et₂O.

MS spectrometry: Exact mass determination was carried out on a 6545 Q-ToF (Agilent GmbH, Waldbronn) using Electrospray Ionization (ESI) or Atmospheric Pressure Photoionization (APPI) and sample loop inlet. Mass calibration was carried out on the day of analysis (ESI)/directly before analysis (APPI) using an external standard mixture. FD mass spectra were recorded on a double focusing sectorfield MS MAT95 (Thermo-Finnigan-MAT, Bremen, Germany) using a push rod inlet. Emitters loaded with samples dissolved in CHCl₃ or CH₂Cl₂ were introduced into the system and heated at a rate of 8.5 mA min⁻¹. Acceleration voltage was 4.7 kV and multiplier voltage was 2.1 kV. Mass spectra were recorded in a mass range of 200-2000 m/z.

Elemental analysis was performed on a Vario Micro Cube (Elementar Analysensysteme, Hanau, Germany).

Melting points were determined with a melting point apparatus SMP 3 (Bibby Stuart Scientific, Stone, UK) and are uncorrected. Heating rate: 1-2 °C/min.

Cyclic voltammetry was performed in an undivided 3-electrode cell under argon atmosphere with a Metrohm 663 VA stand equipped with a μ -Autolab type III potentiostat (Metrohm AG, Herisau, Switzerland). WE: electrode tip (glassy carbon, platinum, boron-doped diamond, isostatic graphite, molybdenum), 2 mm in diameter; CE: glassy carbon rod, RE: Ag/AgNO₃ (silver wire in 0.1 M Bu₄NBF₄/MeCN, 0.01 M AgNO₃, E⁰ = 87 mV vs. FcH/FcH⁺)¹ for measurements in MeCN or dichloromethane or Ag/AgCl (LiCl sat. in EtOH) for measurements in HFIP; v = 50-100 mV/s. Prior to the measurement electrolyte solutions were degassed with argon for at least 5 min.

2. Experimental Setup

The undivided cells are made of Teflon and were used for the screening experiments.² The electrode gap between anode and cathode was approx. 4.8 mm in this setup and the active surface of each planar electrode was 1.8 cm². For the electrochemical reactions the following materials were used as anode: molybdenum (99.9% Mo, Haines & Maassen, Bonn, Germany), glassy carbon (SIGRADUR[®] G, HTW, Thierhaupten, Germany), boron-doped diamond (DIACHEM[®], 15 μ m boron-doped diamond layer on 3 mm silicon support, CONDIAS GmbH, Itzehoe, Germany), isostatic graphite (SIGRAFINE[®] V2100, SGL Carbon, Bonn /Bad Godesberg, Germany) and platinum (99.9% Pt, ÖGUSSA GmbH, Wien, Austria). As cathode material platinum was used and as power source a multi-channel galvanostat was employed.² This set-up can be commercially purchased from IKA-Werke GmbH & CO KG, Staufen, Germany, as IKA Screening System.

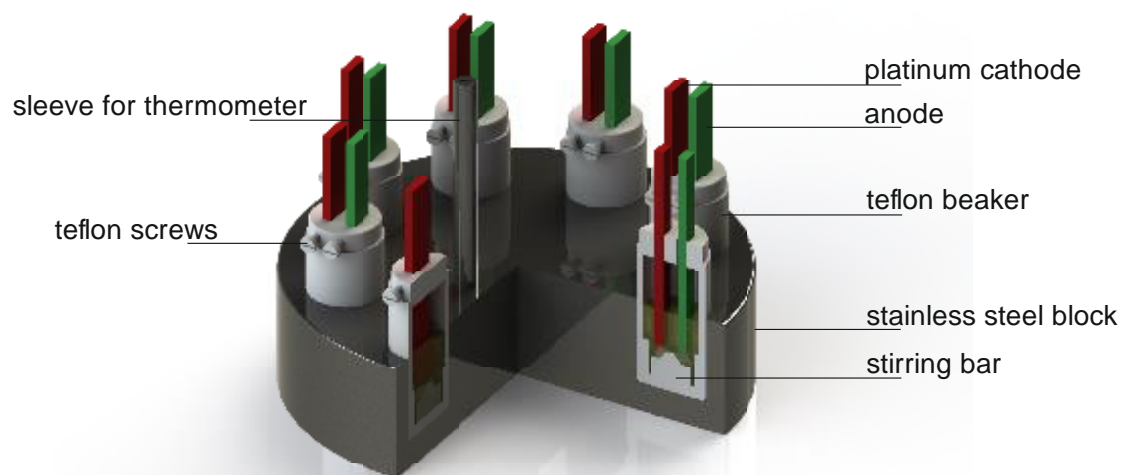


Figure S1: Screening set-up equipped with undivided cells; electrode gap: 4.8 mm; active surface of each planar electrode: 1.8 cm².²

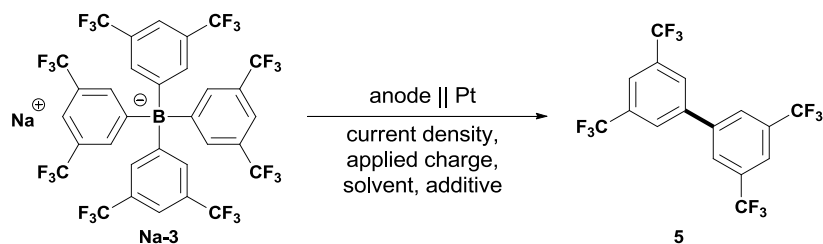
3. General Protocol for the Electrochemical Biphenyl Synthesis from Tetraphenylborates

The biphenyl synthesis from tetraphenylborates was performed in undivided Teflon cells (see Experimental Setup) under constant current (galvanostatic) conditions at room temperature. Unless stated otherwise a current density of 8.3 mA/cm² was applied. If the applied voltage, according to instrumentation, reached the voltage limit of the galvanostat, the current density gradually decreased, which is indicated in the respective tables. The applied charge ranges from 0.68 F to 3.0 F and is specified in the corresponding tables. If the current density reached 0 mA/cm², electrolyses were stopped before the intended applied charge was reached. In this case the actual applied charge is stated. As anode material ($A = 1.8 \text{ cm}^2$) molybdenum, boron-doped diamond, isostatic graphite, glassy carbon, or platinum were employed. As cathode material a platinum plate ($A = 1.8 \text{ cm}^2$) was used in all experiments. The electrolyte consisted of the tetraphenylborates salt (0.5 mmol, 1 eq., $c = 0.1 \text{ M}$) in 5 mL solvent or solvent mixtures. After completion of the electrolysis the reaction mixture was analyzed by GC, GC-MS, and TLC. The crude product was dissolved in ethyl acetate, adsorbed onto silica gel 60 M and purified by silica flash column chromatography (cyclohexane).

4. Optimization of the Electrolysis Parameters

a) Electrochemical Synthesis of 3,3',5,5'-Tetrakis(trifluoromethyl)biphenyl (**5**) from Sodium Tetrakis(3,5-di(trifluoromethyl))phenyl)borate (**Na-3**)

Using sodium tetrakis(3,5-di(trifluoromethyl))phenyl borate (**Na-3**) in hexafluoroisopropanol (HFIP) as supporting electrolyte in a galvanostatic electrochemical setup for the intended electrochemical coupling of 3,4-dimethoxytoluene³ with a molybdenum anode and a platinum cathode we observed degradation of **Na-3**. The respective fluorinated biphenyl 3,3',5,5'-tetrakis(trifluoromethyl)biphenyl (**5**) was isolated in 39% yield. Electrolyzing the pure solution of **Na-3** in HFIP, biphenyl **5** was obtained in 46% yield (Table S1, Entry 1). In the following, the electrolysis conditions for the synthesis of biphenyl **5** have been optimized with regard to anode material, solvent, current density, applied charge and additives (Scheme S1). The obtained results are displayed in Table S1 to Table S4.



Scheme S1: Optimization of the electrochemical synthesis of 3,3',5,5'-tetrakis(trifluoromethyl)biphenyl (**5**) from sodium tetrakis(3,5-di(trifluoromethyl))phenylborate (**Na-3**).

Since redistilled HFIP, containing traces of water and methanol (see NMR spectra) was used in the previous experiment, the effect of water and methanol on the electrochemical synthesis of biphenyl **5** was investigated (Table S1). It turned out, that only methanol is crucial for the synthesis of **5** (Table S1, Entries 2-4).

Table S1: Influence of water and methanol on the synthesis of 3,3',5,5'-tetrakis(trifluoromethyl)biphenyl (**5**).

Entry	Anode	j [mA/cm ²] ^a	Solvent	Additive (vol%)	Yield of 5 [%] ^b
1	Mo	8.3	HFIP ^c	-	46
2	Mo	5.3	HFIP	-	9
3	Mo	8.3	HFIP	H ₂ O (10)	traces ^d
4	Mo	8.3	HFIP	MeOH (10)	31

Electrolytic Conditions: 0.5 mmol Na[B(C₆H₃(CF₃)₂)₄] (**Na-3**), 5 mL solvent, c(Na[B(C₆H₃(CF₃)₂)₄]) = 0.1 M, undivided cell, platinum cathode, 2.57 F, 22 °C.

a: initial current density decreased during electrolysis due to high applied voltage according to instrumentation, b: isolated yield, c: water and methanol impurities were identified by ¹H NMR spectroscopy (NMR spectra), d: observed by GC-MS.

Besides, different anode materials (platinum, glassy carbon, boron-doped diamond (BDD) and isostatic graphite) were investigated (Table S2). As solvent either pure HFIP or redistilled HFIP, containing traces of methanol and water, were used. Independently to the electrode material, higher yields of **5** were obtained using redistilled HFIP. Regarding the electrode material in both cases the highest yield of **5** was obtained at BDD with 41% (Table S2, Entry 2) and 52% (Table S2, Entry 7), respectively. Isostatic graphite refused to synthesize **5** in pure HFIP (Table S2, Entry 5).

Table S2: Screening of different anode materials for the synthesis of 3,3',5,5'-tetrakis(trifluoromethyl)biphenyl (**5**).

Entry	Anode	j [mA/cm ²]	Solvent	Yield of 5 [%] ^b
1	Mo	5.3 ^a	HFIP	9
2	BDD	8.3 ^a	HFIP	41
3	Pt	8.3 ^a	HFIP	37
4	glassy carbon	8.3 ^a	HFIP	32
5	isostatic graphite	8.3 ^a	HFIP	traces ^d
6	Mo	8.3 ^a	HFIP ^c	46
7	BDD	8.3	HFIP ^c	52
8	Pt	8.3	HFIP ^c	46
9	glassy carbon	8.3	HFIP ^c	39

Electrolytic Conditions: 0.5 mmol Na[B(C₆H₃(CF₃)₂)₄] (**Na-3**), 5 mL solvent, c(Na[B(C₆H₃(CF₃)₂)₄]) = 0.1 M, undivided cell, platinum cathode, 2.57 F, 22 °C.

a: initial current density decreased during electrolysis due to high applied voltage according to instrumentation, b: isolated yield, c: water and methanol impurities were identified by ¹H NMR spectroscopy (NMR spectra), d: observed by GC/MS.

As the methanol and water content in recycled HFIP is slightly varying from sample to sample, different solvents and additives were investigated (Table S3). Via addition of small amounts (up to 1 vol%) of methanol to HFIP, the yield of **5** was increased to 46% (Table S3, Entry 4). Pure MeOH resulted in a poor yield of 13%, whereas MeCN gave an increased yield of 57% (Table S3, Entries 1

and 6). At BDD the best yield of **5** (63%) was obtained in acetonitrile, containing 2 vol% of *tert*-butanol (Table S3, Entry 9). Surprisingly, the use of isostatic graphite, which gave only traces of **5** in HFIP, resulted in an excellent yield of 73% in MeCN (Table S3, Entry 10).

Table S3: Screening of different solvents for the synthesis of 3,3',5,5'-tetrakis(trifluoromethyl)biphenyl (**5**).

Entry	Anode	j [mA/cm ²]	Solvent	Additive (vol%)	Yield of 5 [%] ^b
1	BDD	8.3	MeOH	-	13
2	BDD	8.3 ^a	HFIP	MeOH (0.25)	40
3	BDD	8.3 ^a	HFIP	MeOH (0.5)	42
4	BDD	8.3	HFIP	MeOH (1.0)	46
5	BDD	8.3	HFIP	<i>t</i> -BuOH (2)	36
6	BDD	8.3	MeCN	-	57
7	BDD	8.3	MeCN	MeOH (1.0)	34
8	BDD	8.3	MeCN	MeOH (1.0)	53
9	BDD	8.3	MeCN	<i>t</i> -BuOH (2)	63
10	isostatic graphite	8.3	MeCN	-	73
11	isostatic graphite	8.3	MeCN	<i>t</i> -BuOH (2)	69

Electrolytic Conditions: 0.5 mmol Na[B(C₆H₃(CF₃)₂)₄] (**Na-3**), 5 mL solvent, $c(\text{Na}[\text{B}(\text{C}_6\text{H}_3(\text{CF}_3)_2)_4]) = 0.1$ M, undivided cell, platinum cathode, 2.57 F, 22 °C.

a: initial current density decreased during electrolysis due to high applied voltage according to instrumentation, b: isolated yield.

A further optimization of the current density (Table S4, Entries 2 and 3), applied charge (Table S4, Entries 4 and 5) and substrate concentration (Table S4, Entries 6 and 7) had only limited effect on the formation of **5**.

Table S4: Screening of current density, applied charge and substrate concentration for the synthesis of 3,3',5,5'-tetrakis(trifluoromethyl)biphenyl (**5**).

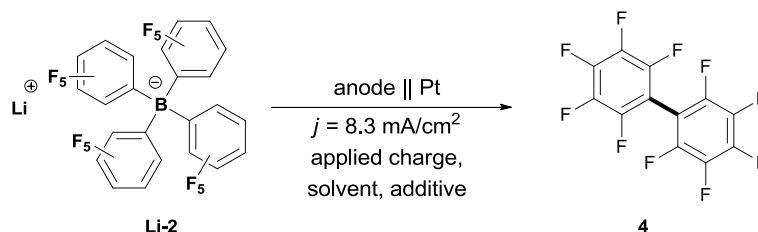
Entry	Anode	j [mA/cm ²]	Q [F]	$c(\text{Na-3})$ [M]	Yield of 5 [%] ^b
1	isostatic graphite	8.3	2.57	0.1	73
2	isostatic graphite	4.2	2.57	0.1	73
3	isostatic graphite	16.6	2.57	0.1	41
4	isostatic graphite	8.3	2.3	0.1	60
5	isostatic graphite	8.3	3.0	0.1	64
6	isostatic graphite	8.3	2.57	0.05	71
7	isostatic graphite	8.3	2.57	0.2	73

Electrolytic Conditions Na[B(C₆H₃(CF₃)₂)₄] (**Na-3**), 5 mL MeCN, undivided cell, platinum cathode, 22 °C.

a: initial current density decreased during electrolysis due to high applied voltage according to instrumentation, b: isolated yield.

We came up with the optimized parameters: isostatic graphite anode, platinum cathode, a current density of 8.3 mA/cm², and an applied charge of 2.57 F in acetonitrile to obtain **5** in 73% isolated yield (Table S3, Entry 10).

b) Electrochemical Synthesis of Decafluorobiphenyl (4) from Lithium Tetrakis(pentafluorophenyl)borate (Li-2)



Scheme S2: Optimization of the electrochemical synthesis of decafluorobiphenyl (**4**) from lithium tetrakis(pentafluorophenyl)borate (**Li-2**).

Applying the original electrolysis conditions, decafluorobiphenyl (**4**) was isolated in a yield of 15% (Table S5, Entry 1). After optimization of the electrolysis conditions for the synthesis of biphenyl **5**, the optimized conditions should be applied for the synthesis of decafluorobiphenyl (**4**). However, only trace amounts of **4** were observed via GC-MS (Table S5, Entry 2). As this is in accordance with the occurrence of side reactions in the cyclic voltammetry measurement at isostatic graphite (Figure S5), BDD and molybdenum were investigated as anode materials (Table S5, Entries 3 to 8). Using MeCN with different additives, still only trace amounts of biphenyl **4** were observed via GS-MS, which could not be isolated.

Table S5: Screening of different electrolytic conditions for the synthesis of decafluorobiphenyl (**4**).

Entry	Anode	j [mA/cm ²]	Solvent	Additive (vol%)	Yield of 4 [%] ^b
1^c	Mo	8.3 ^a	HFIP ^d	-	15
2	isostatic graphite	8.3	MeCN	-	traces ^e
3	BDD	8.3	MeCN	-	traces ^e
4	BDD	8.3	MeCN	<i>t</i> -BuOH (2)	traces ^e
5	BDD	8.3	MeCN	HFIP (20)	traces ^e
6	BDD	8.3	MeCN	MeOH (1)	traces ^e
7	Mo	8.3	MeCN	-	traces ^e
8	Mo	8.3	MeCN	MeOH (1)	traces ^e

Electrolytic Conditions: 0.5 mmol Li[B(C₆F₅)₄] (**Li-2**), 5 mL solvent, c(Li[B(C₆F₅)₄]) = 0.1 M, undivided cell, platinum cathode, 2.57 F, 22 °C.

a: initial current density decreased during electrolysis due to high applied voltage according to instrumentation, b: isolated yield, c: applied charge of 1.86 F, d: water and methanol impurities were identified by ¹H NMR spectroscopy (NMR spectra), e: observed by GC-MS.

Therefore, as solvent again HFIP, containing different amounts of added methanol, was investigated at BDD (Table S6, Entries 1 to 4) and molybdenum (Table S6, Entries 5 to 8) anodes. Although the conductivity of the solution in HFIP was low and the current density decreased during the

electrolysis, due to a highly positive applied voltage according to instrumentation, isolable amounts of decafluorobiphenyl (**4**) were formed. For both anode materials, the highest yield of biphenyl **4** was obtained in HFIP containing 1vol% of methanol (Table S6, Entries 3 and 7). At molybdenum, higher yields of **4** (up to 19%) were observed than at BDD.

Table S6: Screening of different methanol contents in HFIP for the synthesis of decafluorobiphenyl (**4**).

Entry	Anode	j [mA/cm ²] ^a	Solvent	Additive (vol%)	Yield of 4 [%] ^b
1	BDD	8.3	HFIP	-	5
2	BDD	8.3	HFIP	MeOH (0.5)	8
3	BDD	8.3	HFIP	MeOH (1)	12
4	BDD	8.3	HFIP	MeOH (2)	10
5	Mo	8.3	HFIP	-	17
6	Mo	8.3	HFIP	MeOH (0.5)	15
7	Mo	8.3	HFIP	MeOH (1)	19
8	Mo	8.3	HFIP	MeOH (2)	8

Electrolytic Conditions: 0.5 mmol Li[B(C₆F₅)₄] (**Li-2**), 5 mL solvent, c(Li[B(C₆F₅)₄]) = 0.1 M, undivided cell, platinum cathode, 2.57 F, 22 °C.

a: initial current density decreased during electrolysis due to high applied voltage according to instrumentation, b: isolated yield.

Finally, different applied charges were screened at molybdenum anodes (Table S7). In a range from 1.8 F to 2.57 F no significant influence on the yield of **4**, isolated in a maximum yield of 20% (Table S7, Entry 3), was observed. Investigation of higher applied charges was not reasonable, as the current density was already significantly decreased, after a charge of 2.57 F passed.

Table S7: Screening of the applied charge for the synthesis of decafluorobiphenyl (**4**).

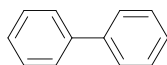
Entry	Anode	j [mA/cm ²] ^a	Q [F]	Solvent	Additive (vol%)	Yield of 4 [%] ^b
1	Mo	8.3	1.8	HFIP	MeOH (1)	10
2	Mo	8.3	2.0	HFIP	MeOH (1)	19
3	Mo	8.3	2.2	HFIP	MeOH (1)	20
4	Mo	8.3	2.57	HFIP	MeOH (1)	19

Electrolytic Conditions: 0.5 mmol Li[B(C₆F₅)₄] (**Li-2**), 5 mL solvent, c(Li[B(C₆F₅)₄]) = 0.1 M, undivided cell, platinum cathode, 22 °C.

a: initial current density decreased during electrolysis, b: isolated yield.

5. Characterization of Biphenyls

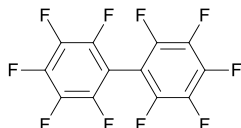
Biphenyl



According to the General Protocol, 280 mg (0.50 mmol, 1 eq.) tetrabutylammonium tetraphenylborate (NBu₄-1) in 5 mL acetonitrile were subjected to electrolysis at an isostatic graphite anode. The electrolysis was performed at 8.3 mA/cm² and a charge of 2.57 F was applied. The crude product was purified by silica flash column chromatography (cyclohexane). Biphenyl was obtained as colorless solid in a yield of 47 mg (0.30 mmol, 61%).

CAS Number: 92-52-4; R_f = 0.62 (99:1 cyclohexane/ethyl acetate); **M.p.:** 68.4-69.8 °C (cyclohexane/ethyl acetate); **¹H NMR** (400 MHz, CDCl₃): δ (ppm) = 7.35-7.42 (m, 2 H), 7.44-7.50 (m, 4 H), 7.61-7.65 (m, 4 H); **¹³C NMR** (101 MHz, CDCl₃): δ (ppm) = 127.3, 127.4, 128.9, 141.4; **MS (FD):** m/z (%) = 154.2 (100%) [M]⁺. The analytical data is in accordance with those reported in literature.⁴

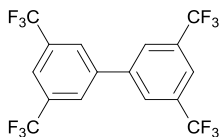
Decafluorobiphenyl (4)



According to the General Protocol, 344 mg (0.50 mmol, 1 eq.) lithium tetrakis(pentafluorophenyl)borate etherate (Li-2) in 5 mL acetonitrile and 50 μ L methanol (1vol%) were subjected to electrolysis at a molybdenum anode. The electrolysis was performed at an initial current density of 8.3 mA/cm². Due to a high applied voltage according to instrumentation (50.4 V) the current density decreased to 1.4 mA/cm² during the electrolysis. A charge of 2.2 F was applied. The crude product was purified by silica flash column chromatography (cyclohexane). Decafluorobiphenyl was obtained as colorless solid in a yield of 33mg (0.10 mmol, 20%).

CAS Number: 434-90-2; R_f = 0.67 (cyclohexane); **¹³C NMR** (151 MHz, CDCl₃): δ (ppm) = 101.4-101.8 (m), 137.9 (dm, J_F = 253.5 Hz), 142.7 (dm, J_F = 258.1 Hz), 144.8 (dm, J_F = 253.4 Hz); **¹⁹F NMR** (376 MHz, CDCl₃): δ (ppm) = -138.6 (m, 4 F), -150.9 (t, J_F = 20.7 Hz, 2 F), -161.4 (m, 4 F); **MS (FD):** m/z (%) = 334.5 (100%) [M]⁺. The analytical data is in accordance with those reported in literature.⁵

3,3',5,5'-Tetrakis(trifluoromethyl)biphenyl (5)



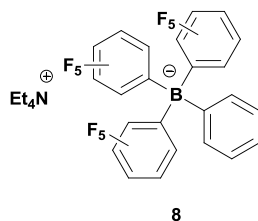
According to the General Protocol, 445 mg (0.50 mmol, 1 eq.) sodium tetrakis(3,5-bis(trifluoromethyl)phenyl)borate (Na-3) in 5 mL acetonitrile were subjected to electrolysis at an isostatic graphite anode. The electrolysis was performed at 8.3 mA/cm² and a charge of 2.57 F was applied. The crude product was purified by silica flash column chromatography (cyclohexane). Biphenyl 5 was obtained as colorless solid in a yield of 156 mg (0.37 mmol, 73%).

CAS Number: 396-44-1; R_f = 0.60 (99:1 cyclohexane/ethyl acetate); **M.p.:** 82.1-83.4 °C (cyclohexane/ethyl acetate); **¹H NMR** (400 MHz, CDCl₃): δ (ppm) = 7.99 (s, 2 H), 8.03 (s, 4 H); **¹³C NMR**

(101 MHz, CDCl₃): δ (ppm) = 122.7-122.9 (m), 123.2 (q, J = 272.9 Hz), 127.5-127.8 (m), 133.1 (q, J = 33.7 Hz), 140.6 (s); ¹⁹F NMR (376 MHz, CDCl₃): δ (ppm) = -64.0 (s); HRMS for C₁₆H₆F₁₂⁺, (APPI), [M]⁺: calc.: 426.0272; found: 426.0268; **Elemental anal.** for C₁₆H₆F₁₂: calc.: C: 45.09%, H: 1.42%, found: C: 44.93%, H: 1.51%. The analytical data is in accordance with those reported in literature.^{4,6}

6. Synthesis of the Unsymmetric Tetraphenyl Borate 7 and Biphenyl 8

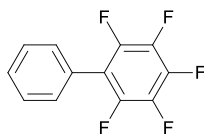
Tetraethylammonium tris(pentafluorophenyl)phenylborate (7)



Tris(pentafluorophenyl)borane (2.56 g, 5.0 mmol, 1.0 eq.) was suspended in anhydrous diethyl ether (20 mL). Phenyl lithium (1.9 M, 3.7 mL, 7.0 mmol, 1.4 eq) was added in one portion at 20 °C and the reaction mixture was stirred for 2 h. The reaction was quenched with water (1 mL) and the solvents were removed under reduced pressure. A saturated solution of sodium carbonate (aq., 60 mL) was added and the aqueous layer was extracted with ethyl acetate (3x 60 mL). The organic layer was dried over sodium sulfate, filtered and the solvent was removed under reduced pressure. The residue was dissolved in dichloromethane (50 mL) and tetraethylammonium chloride (829 mg, 5.0 mmol, 1.0 eq) was added. The mixture was stirred at 20 °C for 1.5 h. The organic layer was washed with water (20 mL) and dried over magnesium sulfate. The solvent was removed under reduced pressure. The crude product was dissolved in dichloromethane (20 mL) and overlaid with diethyl ether (30 mL). The colorless precipitate was collected by filtration (145 mg, 0.20 mmol).¹

¹H NMR (400 MHz, MeCN-*d*₃): δ (ppm) = 7.32-7.22 (m, 2H), 7.00 (t, ³ J = 7.4 Hz, 2H), 6.88-6.82 (m, 1H), 3.14 (q, ³ J = 7.3 Hz, 4H), 1.23-1.17 (m, 6H). ¹³C NMR (101 MHz, MeCN-*d*₃): δ (ppm) = 164.8 (dd, J_F = 98.5, 49.3 Hz), 136.7 (s), 126.6 (dd, J_F = 5.7, 2.8 Hz), 122.8 (s), 53.1-53.0 (m), 7.64 (s).² ¹¹B NMR (128 MHz, MeCN-*d*₃): δ (ppm) = -16.8 (s). ¹⁹F NMR (377 MHz, MeCN-*d*₃): δ (ppm) = -134.7- -135.2 (m, 6F), -165.1 (t, ³ J_{FF} = 19.7 Hz, 3F), -169.5 (t, ³ J_{FF} = 18.9 Hz, 6F). **HR-MS** (ESI): m/z calc. for C₂₄H₅BF₁₅ [M=B(Ph)(C₆F₅)₃]⁻ 589.0250, found 589.0233.

2,3,4,5,6-Pentafluorobiphenyl (8)



According to the General Protocol, 20 mg (0.03 mmol, 1 eq.) Tetraethylammonium tris(pentafluorophenyl)phenylborate (7) in 5 mL acetonitrile were subjected to electrolysis at an

¹ The solids could not be further purified. The formation of the unsymmetrical BARF anion was clearly verified by ESI-MS. Based on the NMR we are convinced that an agglomerate with the formula (Et₄N)⁺[B(Ph)(C₆F₅)₃]₂⁻ is formed most likely. Since full characterization is pending and the reaction is not optimized, we considered the salt as attempted Et₄N⁺[B(Ph)(C₆F₅)₃]⁻ and used this formula for the mechanistic investigation.

² Peaks for carbon-fluorine bonds are of low intensity and not fully resolved.

isostatic graphite anode. The electrolysis was performed at 8.3 mA/cm² and a charge of 2.57 F was applied. The reaction mixture was analyzed by GC-MS.

GC-MS: 7.856 min, m/z = 244 Da.

7. Cyclic Voltammetry Studies

a) Tetraphenylborates as Supporting Electrolyte

Cyclic voltammograms of 0.1 M solutions of Bu_4NBPh_4 (**Bu₄N-1**), $\text{Na}[\text{B}(\text{C}_6\text{H}_3(\text{CF}_3)_2)_4]$ (**Na-3**) and $\text{Li}[\text{B}(\text{C}_6\text{F}_5)_4]$ (**Li-2**) in acetonitrile were recorded at boron-doped diamond (BDD), glassy carbon, platinum, and isostatic graphite working electrodes (Figure S2 to Figure S5). At glassy carbon, platinum, and boron-doped diamond the anodic limit potential was determined as the potential at which the current density exceeded 1 mA/cm^2 (Table S8). Due to the increased background current at isostatic graphite, in this case the potential at which the current density exceeded 3 mA/cm^2 was determined as anodic potential limit.

Cyclic voltammograms of 0.1 M solutions of $\text{Li}[\text{B}(\text{C}_6\text{F}_5)_4]$ (**Li-2**) in 1,1,1,3,3,3-hexafluoroisopropanol (HFIP) and HFIP + 1vol% methanol were measured at a molybdenum working electrode (Figure S6 to Figure S7).

Table S8: Anodic limit potential of tetraphenylborate salts **1-3** in acetonitrile at different working electrode materials. Potentials given vs. FcH/FcH^+ ; a: cut-off current density = 1.5 mA/cm^2 , due to high background current; b: cut-off current density = 1.5 mA/cm^2 , due to low background current.

Working Electrode	NBu_4BPh_4 (Bu₄N-1)	$\text{Na}[\text{B}(\text{C}_6\text{H}_3(\text{CF}_3)_2)_4]$ (Na-3)	$\text{Li}[\text{B}(\text{C}_6\text{F}_5)_4]$ (Li-2)
BDD	0.49 V	1.64 V	1.63 V
glassy carbon	0.28 V	1.52 V	1.78 V
platinum	0.37 V	1.51 V ^a	1.68 V
isostatic graphite	0.17 V ^b	1.25 V	-

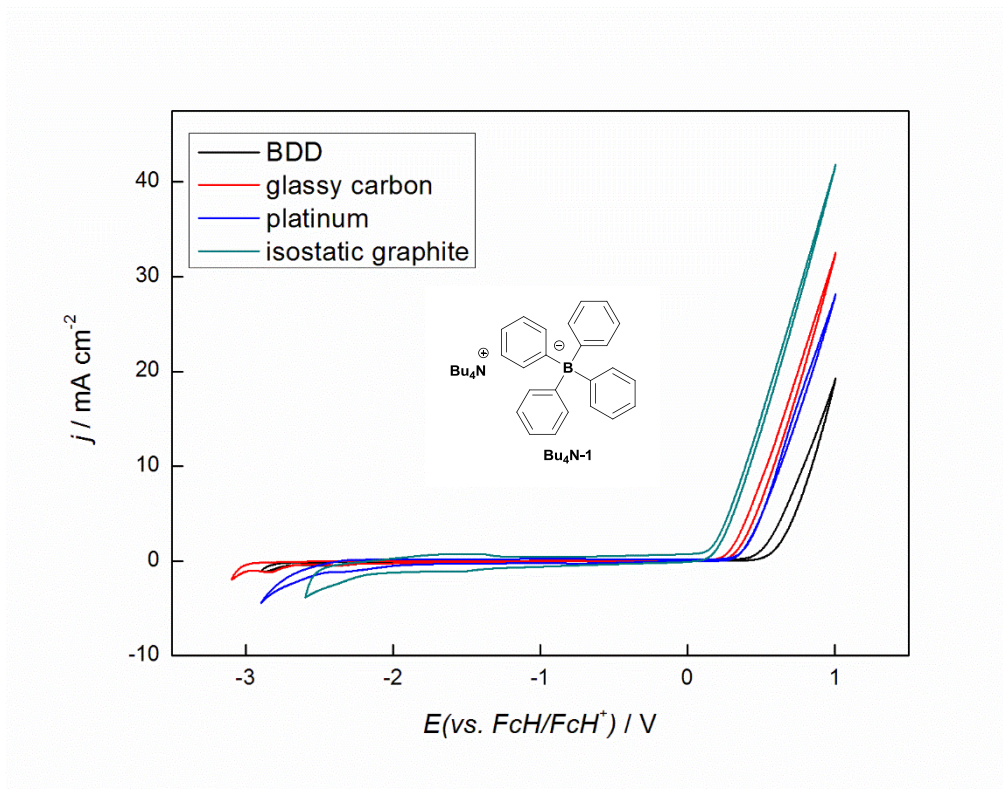


Figure S2: Cyclic voltammograms of 0.1 M Bu_4NBPh_4 (**Bu₄N-1**)/MeCN, working electrode: boron-doped diamond (BDD, black line), glassy carbon (red line), platinum (blue line), isostatic graphite (green line), scan rate: 100 mV/s.

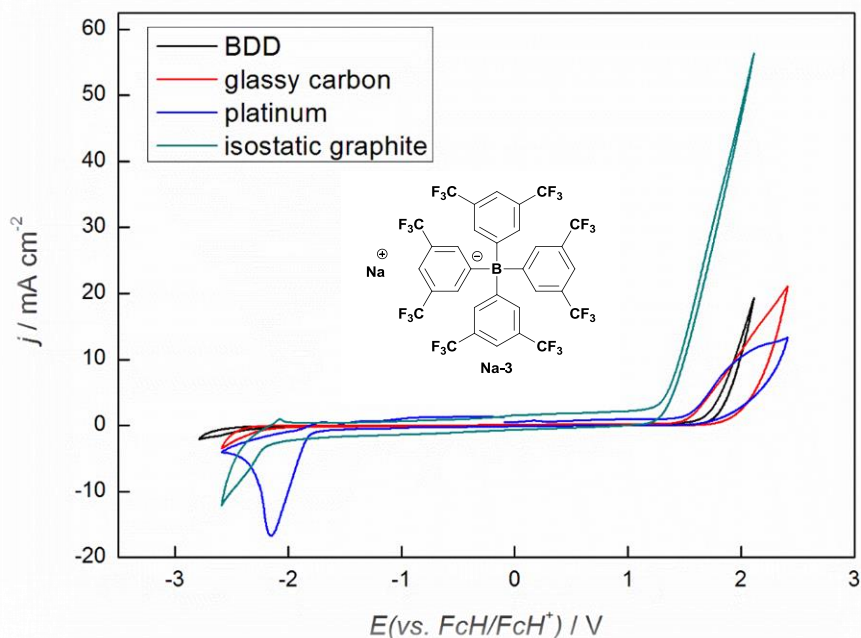


Figure S3: Cyclic voltammograms of 0.1 M $\text{Na}[\text{B}(\text{C}_6\text{H}_3(\text{CF}_3)_2)_4]$ (**Na-3**)/MeCN, working electrode: boron-doped diamond (BDD, black line), glassy carbon (red line), platinum (blue line), isostatic graphite (green line), scan rate: 100 mV/s.

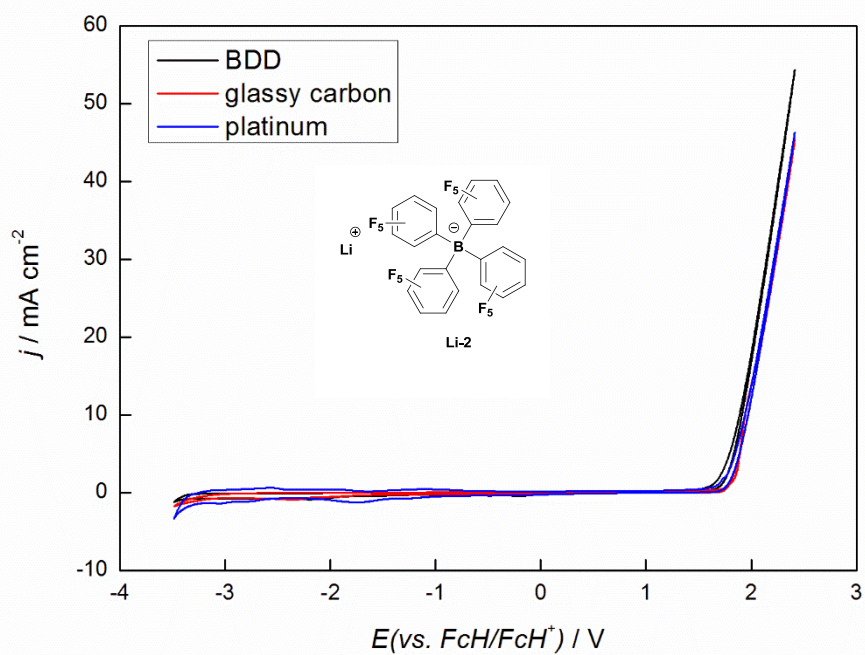


Figure S4: Cyclic voltammograms of 0.1 M Li[B(C₆F₅)₄] (Li-2)/MeCN, working electrode: boron-doped diamond (BDD, black line), glassy carbon (red line), platinum (blue line), scan rate: 100 mV/s.

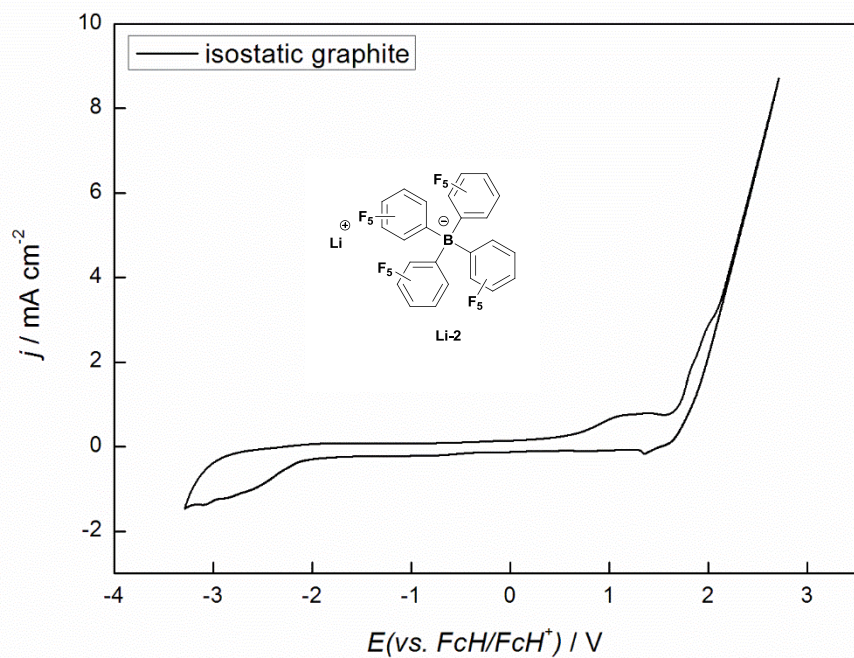


Figure S5: Cyclic voltammograms of 0.1 M Li[B(C₆F₅)₄] (Li-2)/MeCN, working electrode: isostatic graphite, scan rate: 100 mV/s.

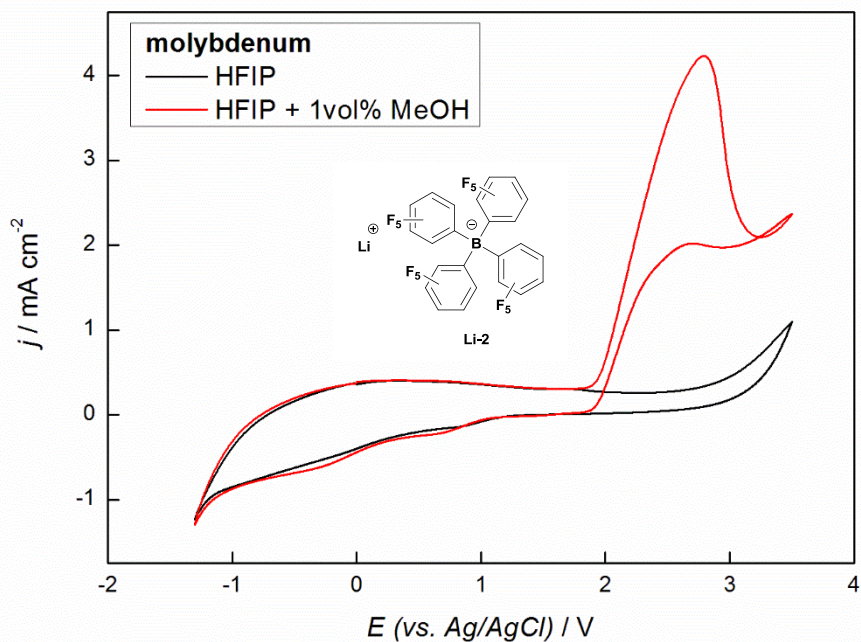


Figure S6: Cyclic voltammograms of 0.1 M $\text{Li}[\text{B}(\text{C}_6\text{F}_5)_4]$ (Li-2)/HFIP (black line), 0.1 M $\text{Li}[\text{B}(\text{C}_6\text{F}_5)_4]$ (Li-2)/HFIP+1vol% MeOH (red line), working electrode: molybdenum, scan rate: 100 mV/s.

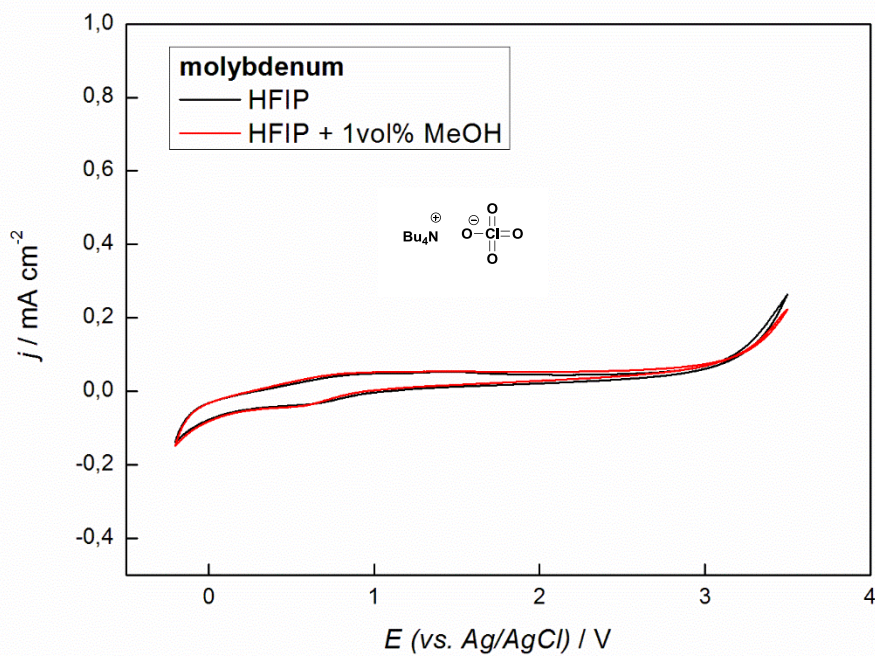


Figure S7: Cyclic voltammograms of 0.1 M Bu_4NClO_4 /HFIP (black line), 0.1 M Bu_4NClO_4 /HFIP+1vol% MeOH (red line), working electrode: molybdenum, scan rate: 100 mV/s.

b) Tetraphenylborates as Substrates

Cyclic voltammograms of 3 mM Bu_4NBPh_4 (**Bu₄N-1**), $\text{Na}[\text{B}(\text{C}_6\text{H}_3(\text{CF}_3)_2)_4]$ (**Na-3**), $\text{Li}[\text{B}(\text{C}_6\text{F}_5)_4]$ (**Li-2**) and biphenyl in 0.1 M $\text{Bu}_4\text{NClO}_4/\text{CH}_2\text{Cl}_2$ or 0.1 M $\text{NaClO}_4/\text{MeCN}$ were measured at boron-doped diamond (BDD), glassy carbon, platinum and molybdenum working electrodes (Figures S8-S33).

Table S9: Oxidation potentials (E^{ox}) of tetraphenylborate salts **1-3** in 0.1 M $\text{Bu}_4\text{NClO}_4/\text{CH}_2\text{Cl}_2$ or 0.1 M $\text{NaClO}_4/\text{MeCN}$ at different working electrode materials. Potentials given vs. FcH/FcH^+ ; values in brackets: peak potentials in the 2nd or 3rd cycle; a: conversion constant from SCE to FcH/FcH^+ according to Pavlishchuk and Addison: 380 mV.¹ b: No clear oxidation peak identified.

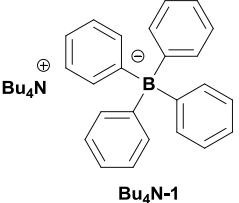
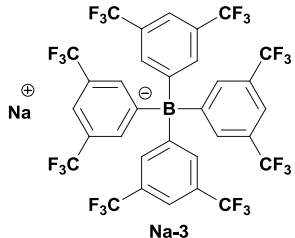
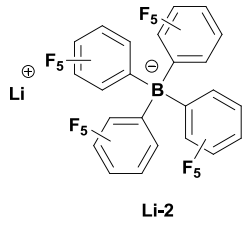
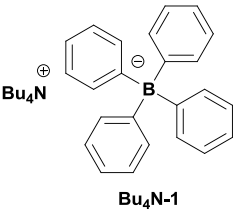
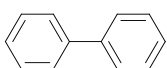
tetraphenylborate salt	electrolyte	BDD	glassy carbon	platinum
 Bu₄N-1	0.1 M $\text{Bu}_4\text{NClO}_4/\text{CH}_2\text{Cl}_2$	0.88 V	0.39 V	0.65 V (2 nd : 0.57 V)
	Datta <i>et al.</i> ⁷ : 0.1 M $\text{Bu}_4\text{NClO}_4/\text{CH}_2\text{Cl}_2$	-	0.89 V vs. SCE ⁷ 0.51 V ^a	0.87 V vs. SCE ⁷ 0.49 V ^a
	0.1 M $\text{NaClO}_4/\text{MeCN}$	0.93 V (2 nd : 0.99 V) (3 rd : 1.09 V)	0.48 V (2 nd : 0.64 V)	0.57 V (2 nd : 0.49 V) (3 rd : 0.47 V)
	Datta <i>et al.</i> ⁷ : 0.1 M $\text{NaClO}_4/\text{MeCN}$	-	0.78 V vs. SCE ⁷ 0.40 V ^[a]	0.85 V vs. SCE ⁷ 0.47 V ^[a]
 Na-3	0.1 M $\text{Bu}_4\text{NClO}_4/\text{CH}_2\text{Cl}_2$	1 st /2 nd /3 rd : shoulder at 2.0 V	shoulder at 1.7-1.8 V	1.57 V (2 nd /3 rd : shoulder at 1.55 V)
	0.1 M $\text{NaClO}_4/\text{MeCN}$	1.56 V	shoulder at 1.9 V	2.02 V (2 nd : 1.96 V) (3 rd : 1.95 V)
 Li-2	0.1 M $\text{Bu}_4\text{NClO}_4/\text{CH}_2\text{Cl}_2$	shoulder ^b	shoulder ^b	shoulder ^b
	0.1 M $\text{NaClO}_4/\text{MeCN}$	shoulder at 2.1 V	1.83 V (2 nd peak: 2.33 V)	shoulder at 2.0 V (2 nd and 3 rd : shoulder at 1.9 V)

Table S10: 2nd Oxidation peak (E^{Ox}) in the cyclic voltammogram of Bu_4NBPh_4 (**1**) and oxidation potential (E^{Ox}) of biphenyl in 0.1 M Bu_4NClO_4/CH_2Cl_2 or 0.1 M $NaClO_4/MeCN$ at different working electrode materials. Potentials given vs. FcH/FcH^+ ; values in brackets: peak potentials in the 2nd or 3rd cycle.

tetraphenylborate salt	electrolyte	BDD	glassy carbon	platinum
 Bu_4N-1	0.1 M Bu_4NClO_4/CH_2Cl_2	1.56 V (2 nd : 1.62 V)	1.61 V (2 nd : 1.51 V)	1.60 V (2 nd : 1.49 V) (3 rd : 1.53 V)
	0.1 M $NaClO_4/MeCN$	1.52 V (2 nd : 1.56 V) (3 rd : 1.55 V)	1.51 V (2 nd : 1.52 V) (3 rd : 1.55 V)	1.50 V (2 nd : 1.50 V) (3 rd : 1.50 V)
	0.1 M Bu_4NClO_4/CH_2Cl_2	1.59 V	1.68 V	1.67 V
	0.1 M $NaClO_4/MeCN$	1.50 V	1.50 V	1.50 V

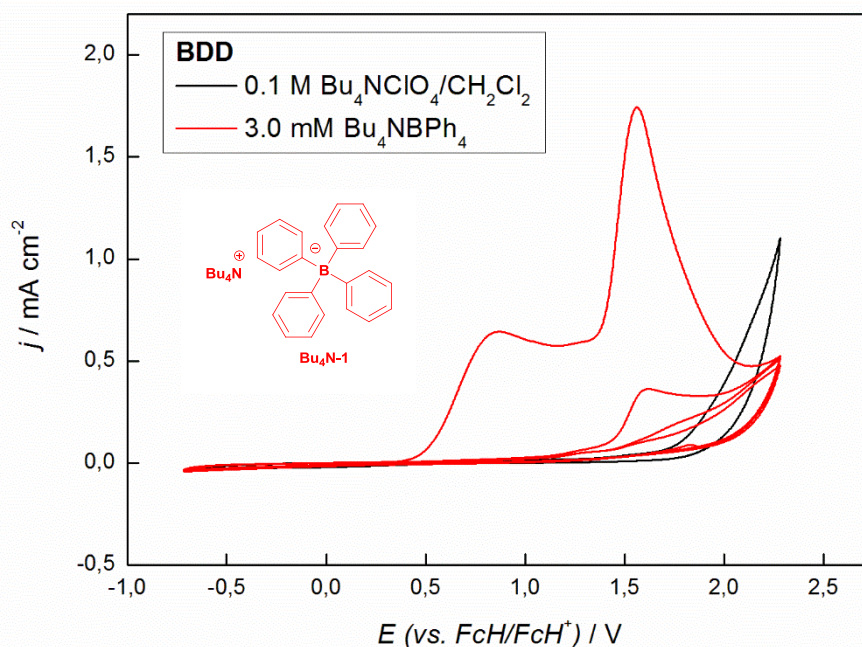


Figure S8: Cyclic voltammogram of 0.1 M Bu_4NClO_4/CH_2Cl_2 (black line) and 3.0 mM Bu_4NBPh_4 (Bu_4N-1) (red line), working electrode: BDD, electrolyte: 0.1 M Bu_4NClO_4/CH_2Cl_2 , scan rate: 50 mV/s.

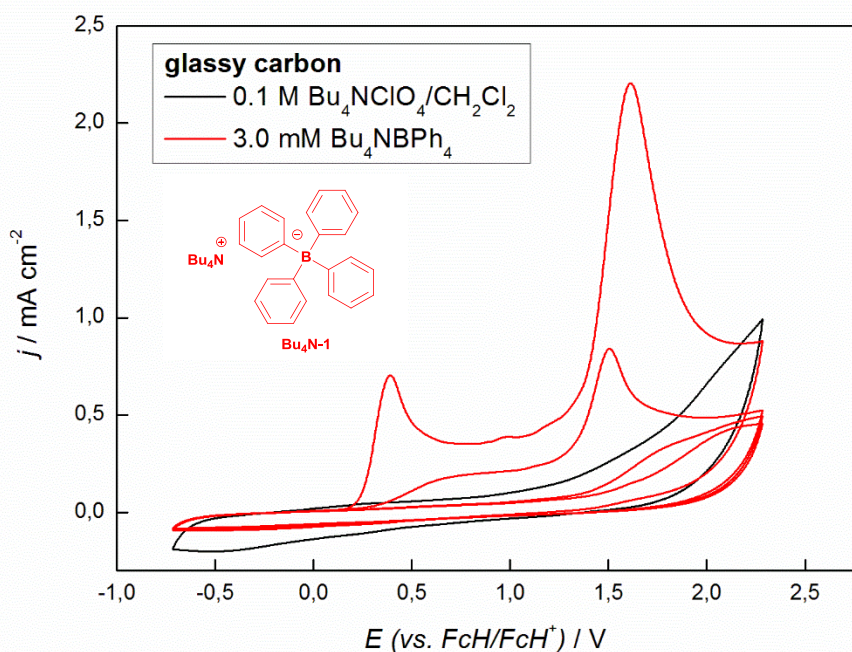


Figure S9: Cyclic voltammogram of 0.1 M $\text{Bu}_4\text{NClO}_4/\text{CH}_2\text{Cl}_2$ (black line) and 3.0 mM Bu_4NBPh_4 ($\text{Bu}_4\text{N-1}$) (red line), working electrode: glassy carbon, electrolyte: 0.1 M $\text{Bu}_4\text{NClO}_4/\text{CH}_2\text{Cl}_2$, scan rate: 50 mV/s.

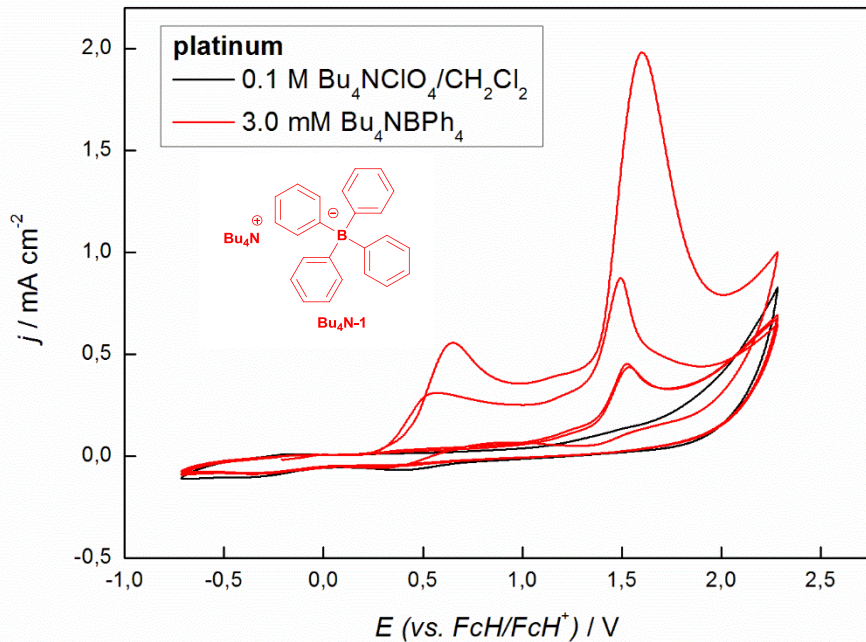


Figure S10: Cyclic voltammogram of 0.1 M $\text{Bu}_4\text{NClO}_4/\text{CH}_2\text{Cl}_2$ (black line) and 3.0 mM Bu_4NBPh_4 ($\text{Bu}_4\text{N-1}$) (red line), working electrode: platinum, electrolyte: 0.1 M $\text{Bu}_4\text{NClO}_4/\text{CH}_2\text{Cl}_2$, scan rate: 50 mV/s.

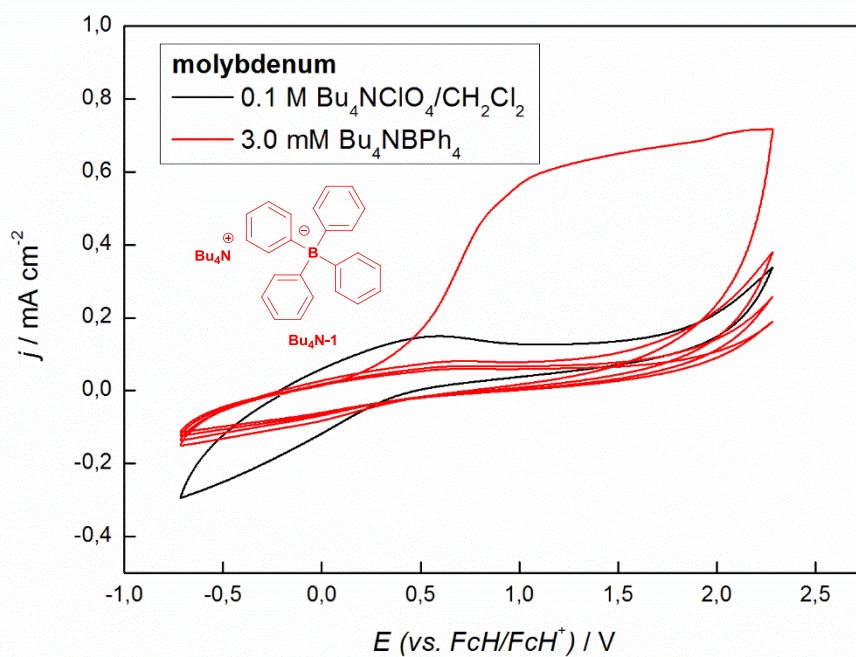


Figure S11: Cyclic voltammogram of 0.1 M $\text{Bu}_4\text{NClO}_4/\text{CH}_2\text{Cl}_2$ (black line) and 3.0 mM Bu_4NBPh_4 ($\text{Bu}_4\text{N-1}$) (red line), working electrode: molybdenum, electrolyte: 0.1 M $\text{Bu}_4\text{NClO}_4/\text{CH}_2\text{Cl}_2$, scan rate: 50 mV/s.

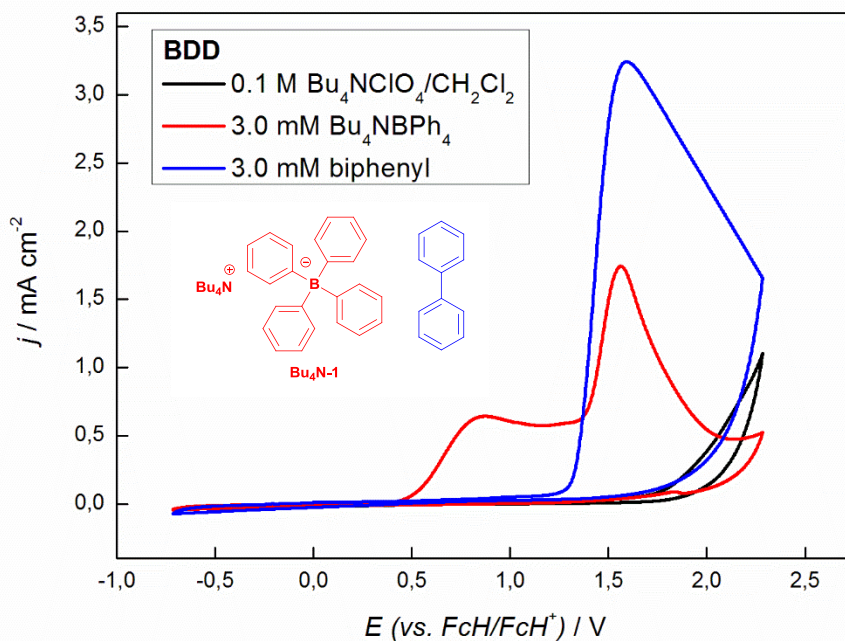


Figure S12: Cyclic voltammograms of 0.1 M $\text{Bu}_4\text{NClO}_4/\text{CH}_2\text{Cl}_2$ (black line), 3.0 mM Bu_4NBPh_4 ($\text{Bu}_4\text{N-1}$) (red line) and 3.0 mM biphenyl (blue line), working electrode: BDD, electrolyte: 0.1 M $\text{Bu}_4\text{NClO}_4/\text{CH}_2\text{Cl}_2$, scan rate: 50 mV/s.

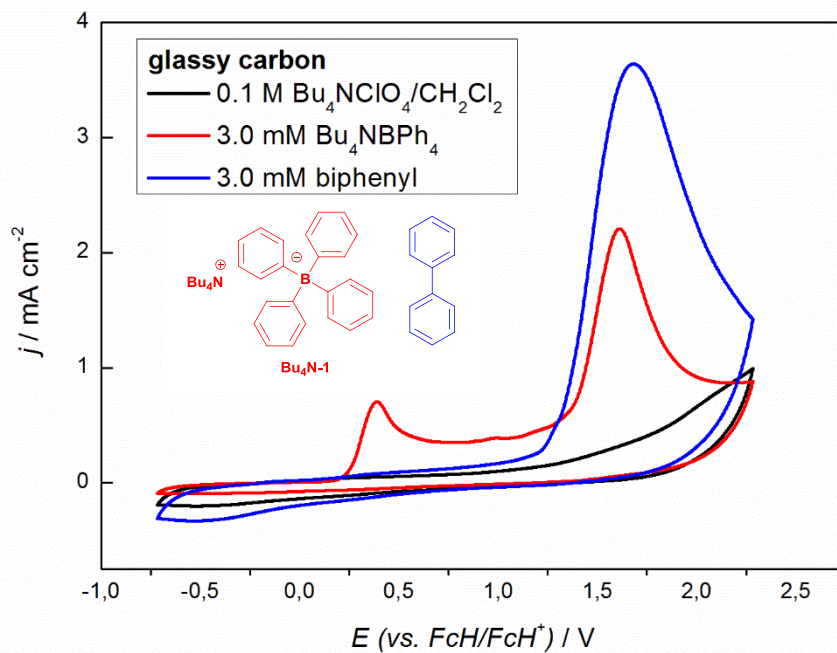


Figure S13: Cyclic voltammograms of 0.1 M $\text{Bu}_4\text{NClO}_4/\text{CH}_2\text{Cl}_2$ (black line), 3.0 mM Bu_4NBPh_4 ($\text{Bu}_4\text{N-1}$) (red line) and 3.0 mM biphenyl (blue line), working electrode: glassy carbon, electrolyte: 0.1 M $\text{Bu}_4\text{NClO}_4/\text{CH}_2\text{Cl}_2$, scan rate: 50 mV/s.

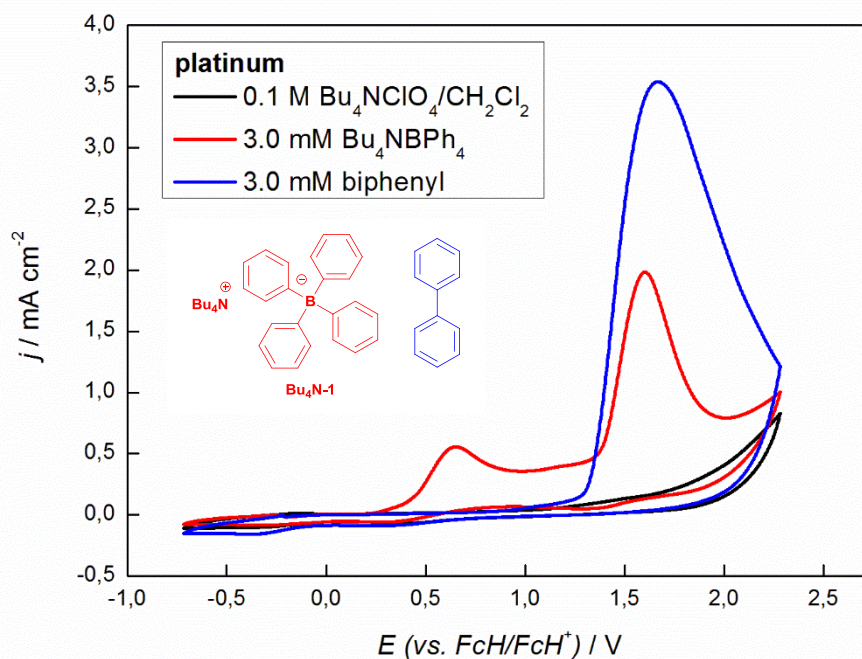


Figure S14: Cyclic voltammograms of 0.1 M $\text{Bu}_4\text{NClO}_4/\text{CH}_2\text{Cl}_2$ (black line), 3.0 mM Bu_4NBPh_4 ($\text{Bu}_4\text{N-1}$) (red line) and 3.0 mM biphenyl (blue line), working electrode: platinum, electrolyte: 0.1 M $\text{Bu}_4\text{NClO}_4/\text{CH}_2\text{Cl}_2$, scan rate: 50 mV/s.

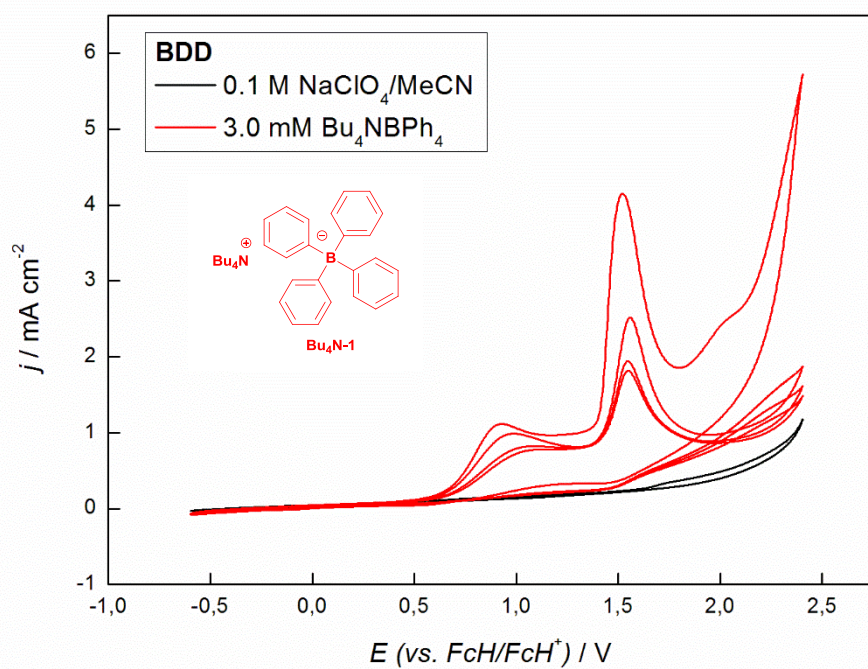


Figure S15: Cyclic voltammogram of 0.1 M NaClO₄/MeCN and 3.0 mM Bu₄NBPh₄ (Bu₄N-1), working electrode: BDD, electrolyte: 0.1 M NaClO₄/MeCN, scan rate: 50 mV/s.

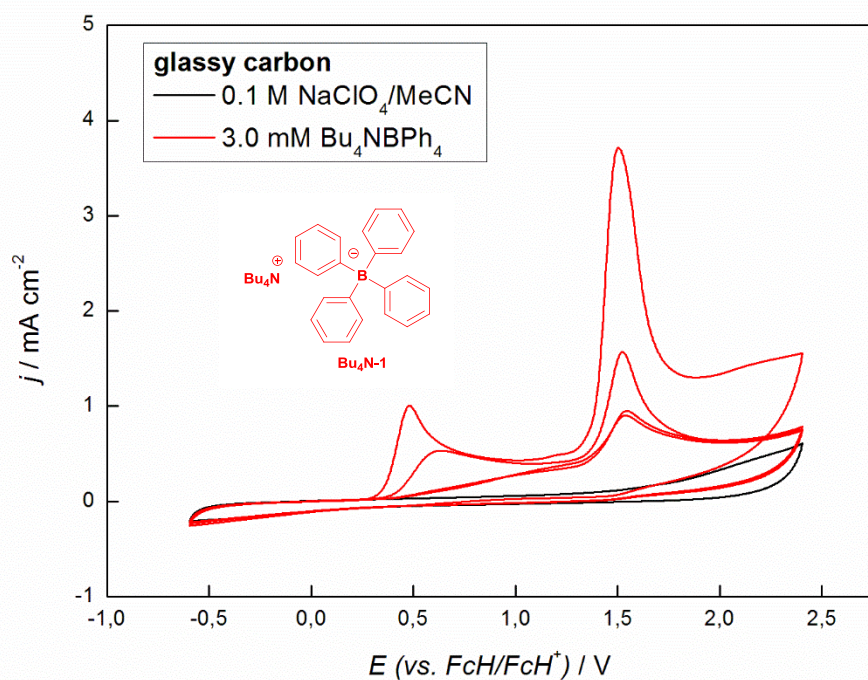


Figure S16: Cyclic voltammogram of 0.1 M NaClO₄/MeCN and 3.0 mM Bu₄NBPh₄ (Bu₄N-1), working electrode: glassy carbon, electrolyte: 0.1 M NaClO₄/MeCN, scan rate: 50 mV/s.

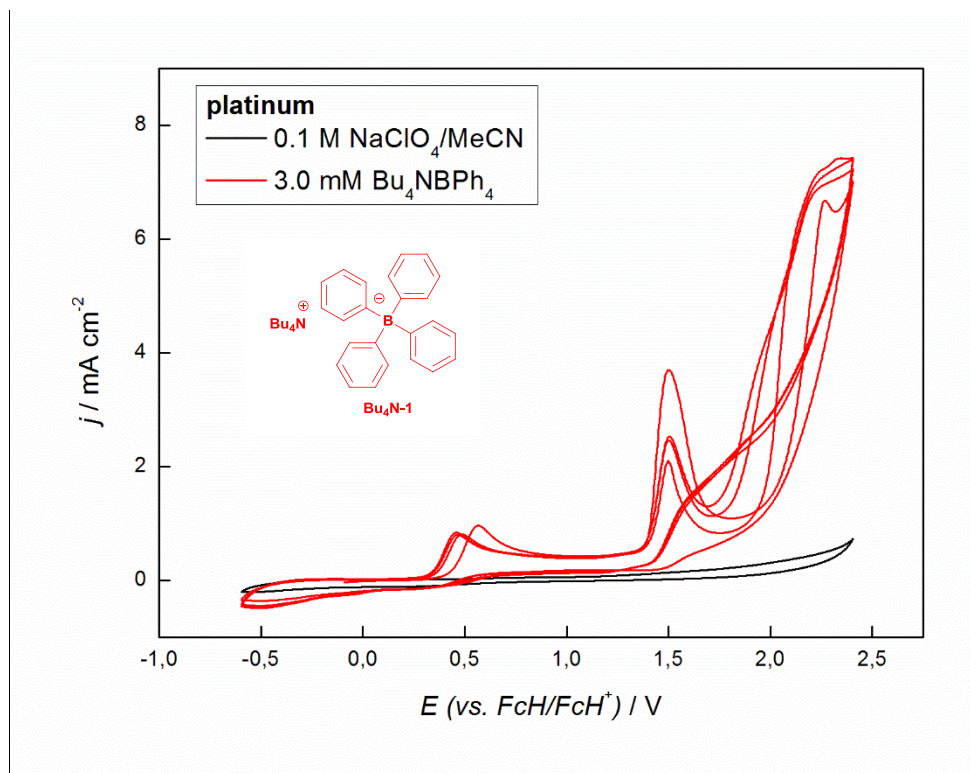


Figure S17: Cyclic voltammogram of 0.1 M $\text{NaClO}_4/\text{MeCN}$ and 3.0 mM Bu_4NBPh_4 ($\text{Bu}_4\text{N-1}$), working electrode: platinum, electrolyte: 0.1 M $\text{NaClO}_4/\text{MeCN}$, scan rate: 50 mV/s.

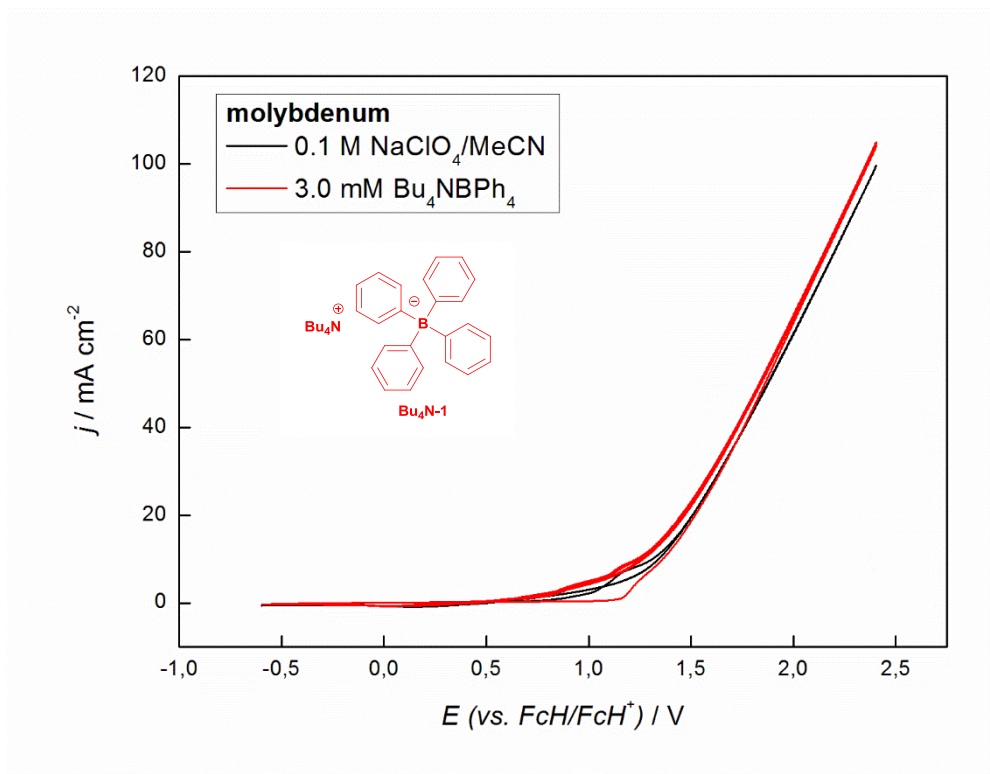


Figure S18: Cyclic voltammogram of 0.1 M $\text{NaClO}_4/\text{MeCN}$ and 3.0 mM Bu_4NBPh_4 ($\text{Bu}_4\text{N-1}$), working electrode: molybdenum, electrolyte: 0.1 M $\text{NaClO}_4/\text{MeCN}$, scan rate: 50 mV/s.

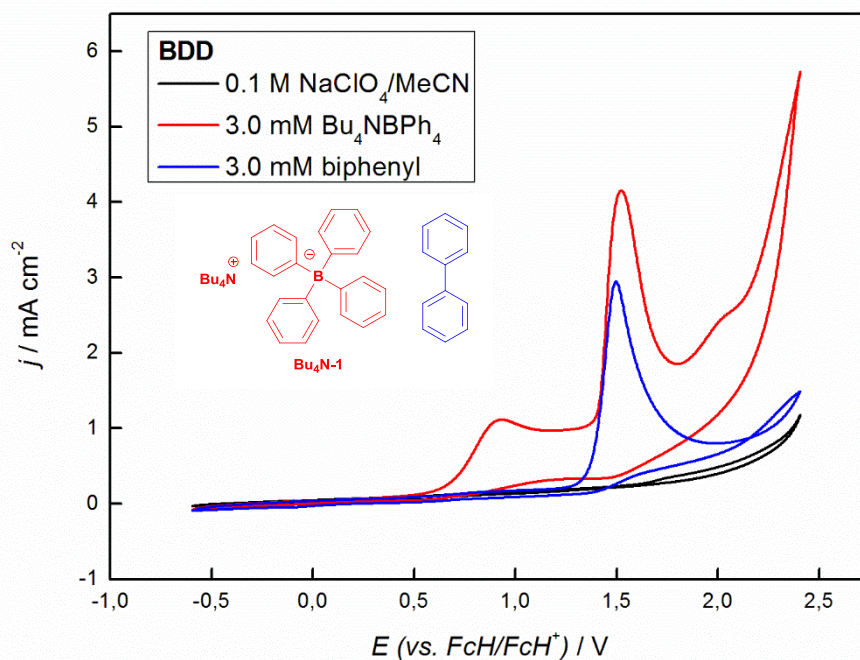


Figure S19: Cyclic voltammograms of 0.1 M NaClO₄/MeCN (black line), 3.0 mM Bu₄NBPh₄ (Bu₄N-1) (red line) and 3.0 mM biphenyl (blue line), working electrode: BDD, electrolyte: 0.1 M NaClO₄/MeCN, scan rate: 50 mV/s.

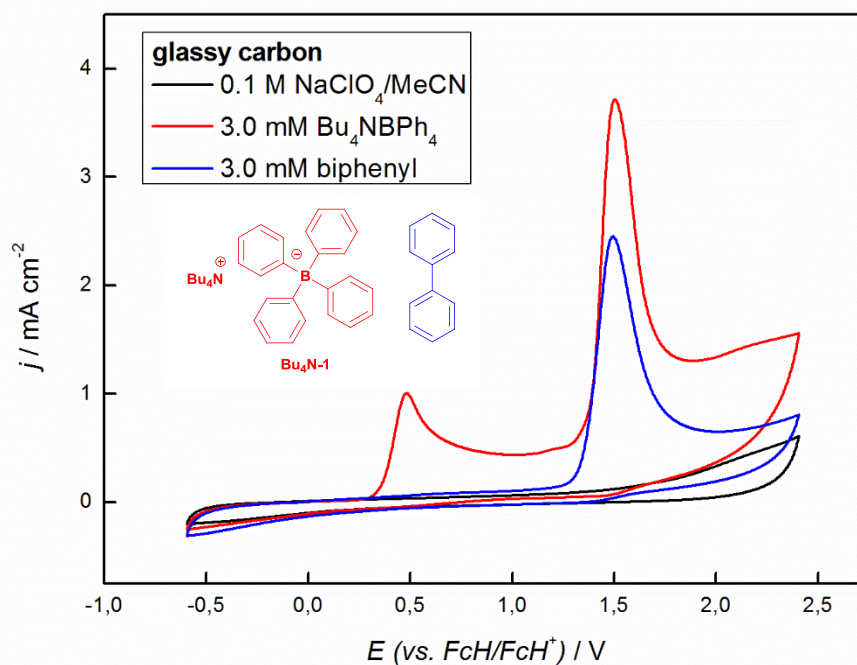


Figure S20: Cyclic voltammograms of 0.1 M NaClO₄/MeCN (black line), 3.0 mM Bu₄NBPh₄ (Bu₄N-1) (red line) and 3.0 mM biphenyl (blue line), working electrode: glassy carbon, electrolyte: 0.1 M NaClO₄/MeCN, scan rate: 50 mV/s.

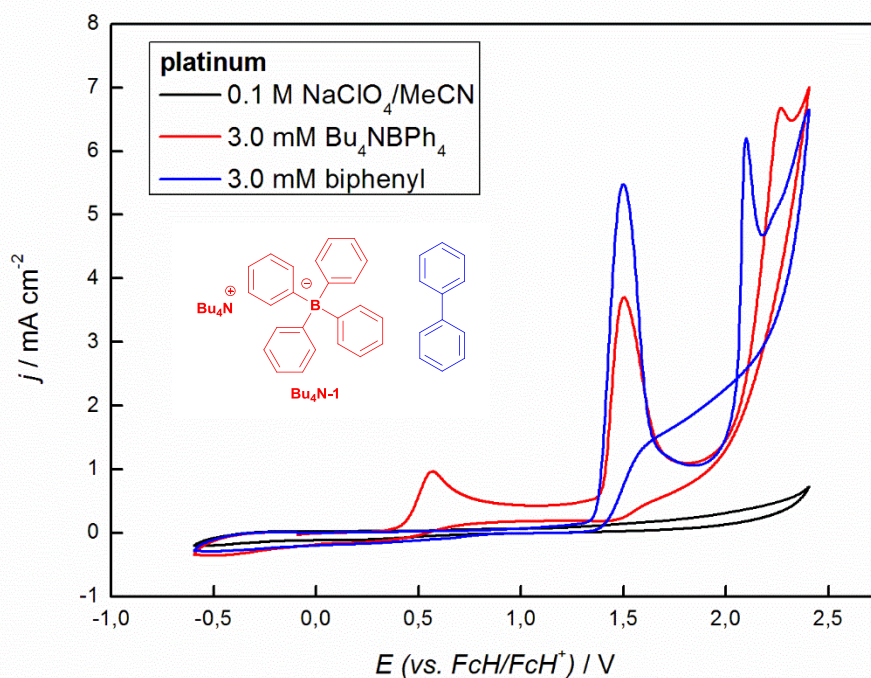


Figure S21: Cyclic voltammograms of 0.1 M NaClO₄/MeCN (black line), 3.0 mM Bu₄NBPh₄ (Bu₄N-1) (red line) and 3.0 mM biphenyl (blue line), working electrode: platinum, electrolyte: 0.1 M NaClO₄/MeCN, scan rate: 50 mV/s.

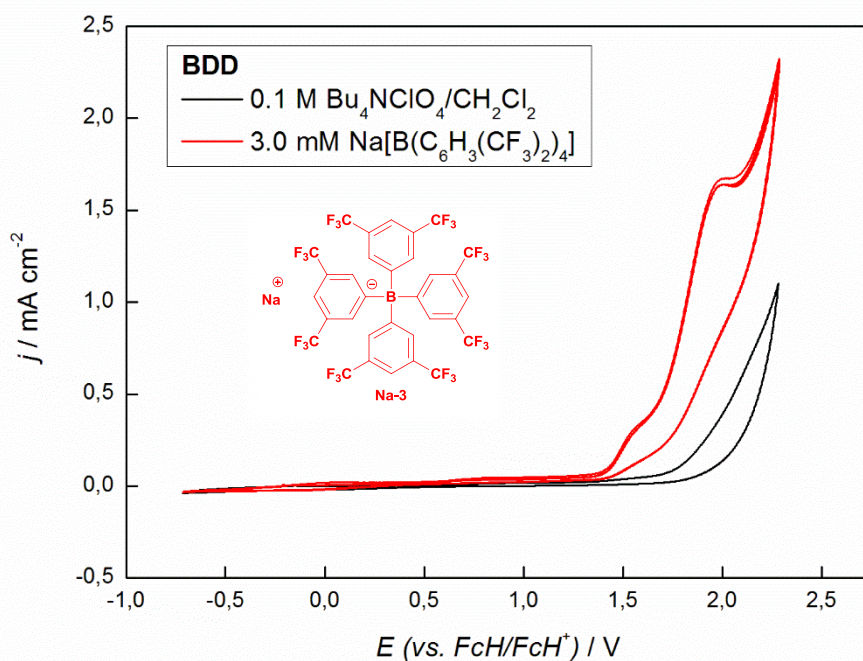


Figure S22: Cyclic voltammogram of 0.1 M Bu₄NClO₄/CH₂Cl₂ (black line) and 3.0 mM Na[B(C₆H₃(CF₃)₂)₄] (Na-3) (red line), working electrode: BDD, electrolyte: 0.1 M Bu₄NClO₄/CH₂Cl₂, scan rate: 50 mV/s.

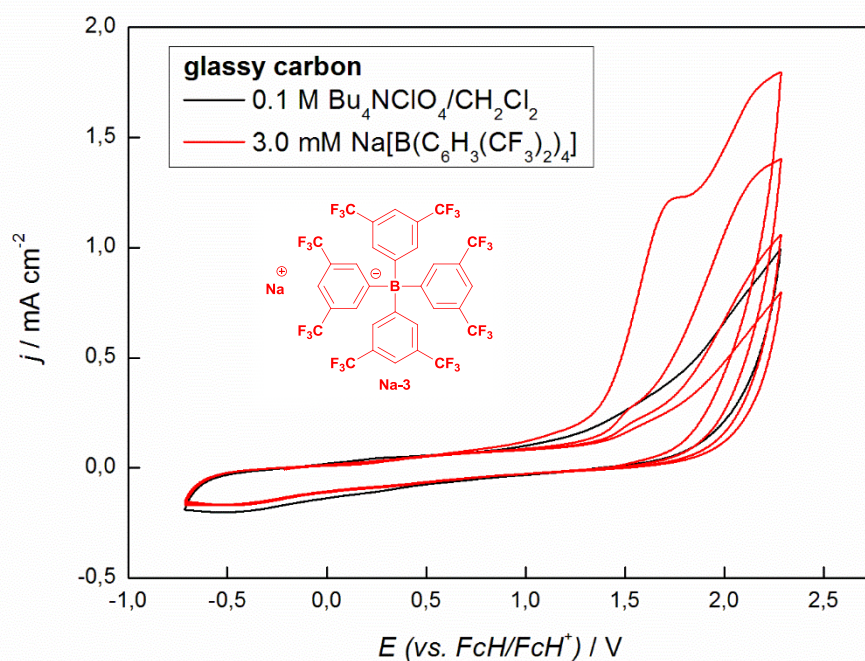


Figure S23: Cyclic voltammogram of 0.1 M $\text{Bu}_4\text{NClO}_4/\text{CH}_2\text{Cl}_2$ (black line) and 3.0 mM $\text{Na}[\text{B}(\text{C}_6\text{H}_3(\text{CF}_3)_2)_4]$ (Na-3) (red line), working electrode: glassy carbon, electrolyte: 0.1 M $\text{Bu}_4\text{NClO}_4/\text{CH}_2\text{Cl}_2$, scan rate: 50 mV/s.

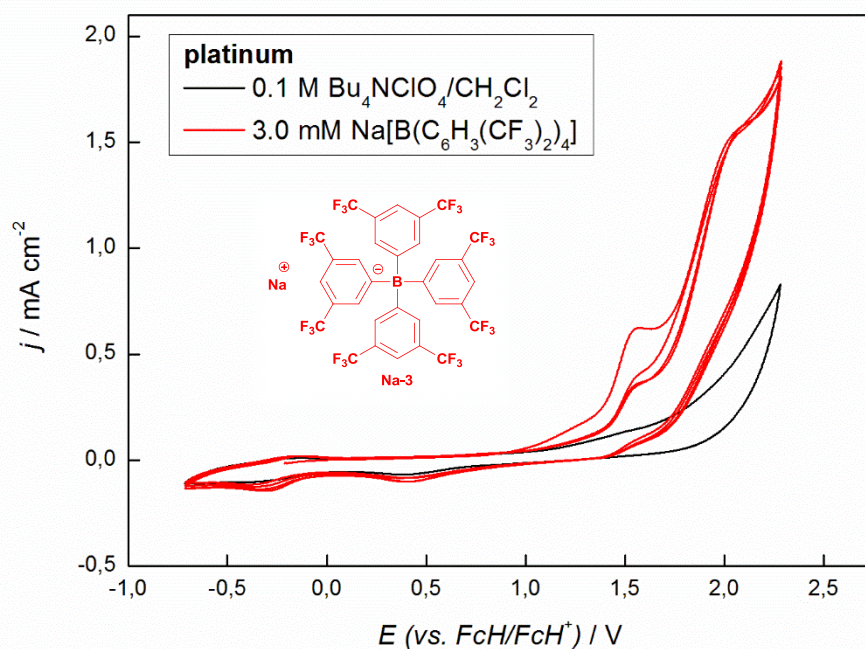


Figure S24: Cyclic voltammogram of 0.1 M $\text{Bu}_4\text{NClO}_4/\text{CH}_2\text{Cl}_2$ (black line) and 3.0 mM $\text{Na}[\text{B}(\text{C}_6\text{H}_3(\text{CF}_3)_2)_4]$ (Na-3) (red line), working electrode: platinum, electrolyte: 0.1 M $\text{Bu}_4\text{NClO}_4/\text{CH}_2\text{Cl}_2$, scan rate: 50 mV/s.

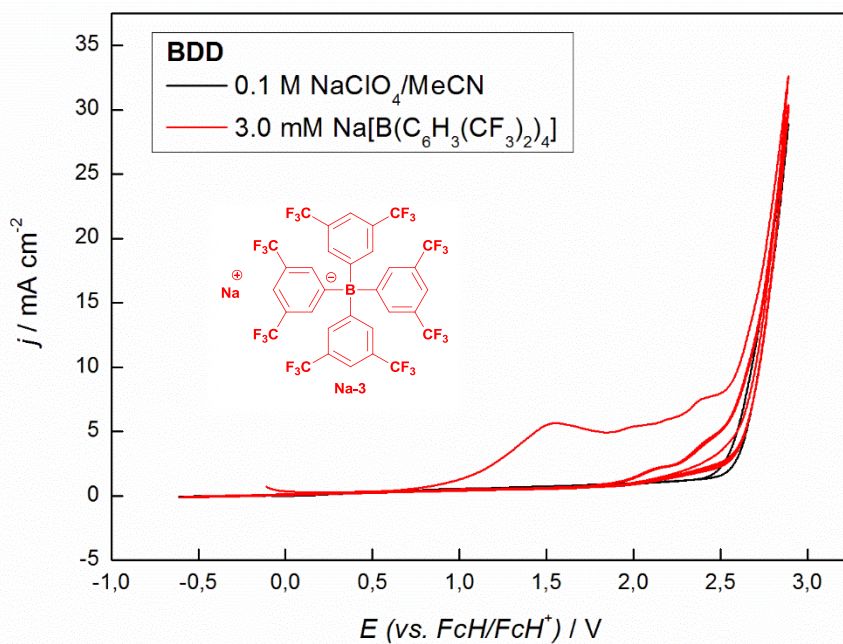


Figure S25: Cyclic voltammogram of 0.1 M NaClO₄/MeCN (black line) and 3.0 mM Na[B(C₆H₃(CF₃)₂)₄] (Na-3) (red line), working electrode: BDD, electrolyte: 0.1 M NaClO₄/MeCN, scan rate: 50 mV/s.

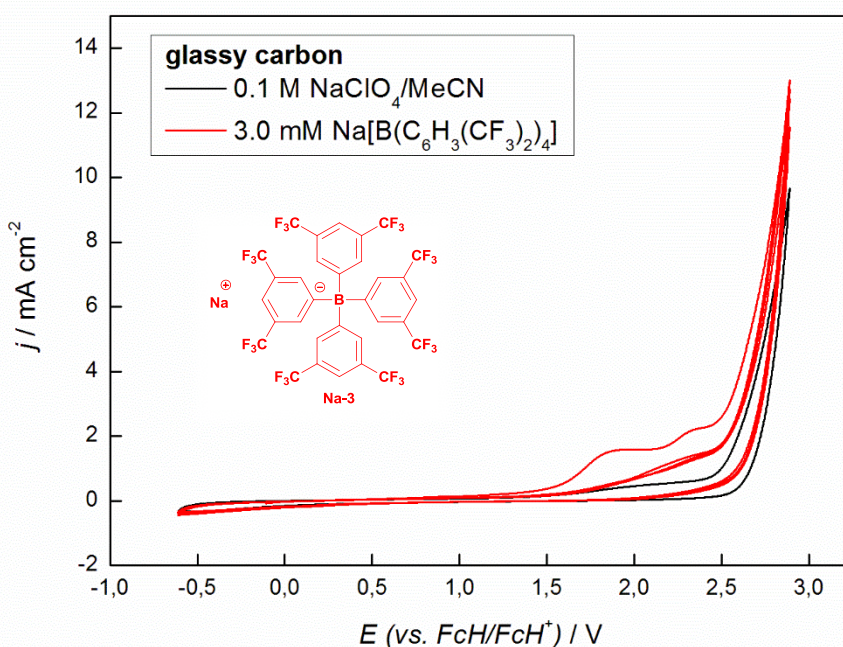


Figure S26: Cyclic voltammogram of 0.1 M NaClO₄/MeCN (black line) and 3.0 mM Na[B(C₆H₃(CF₃)₂)₄] (Na-3) (red line), working electrode: glassy carbon, electrolyte: 0.1 M NaClO₄/MeCN, scan rate: 50 mV/s.

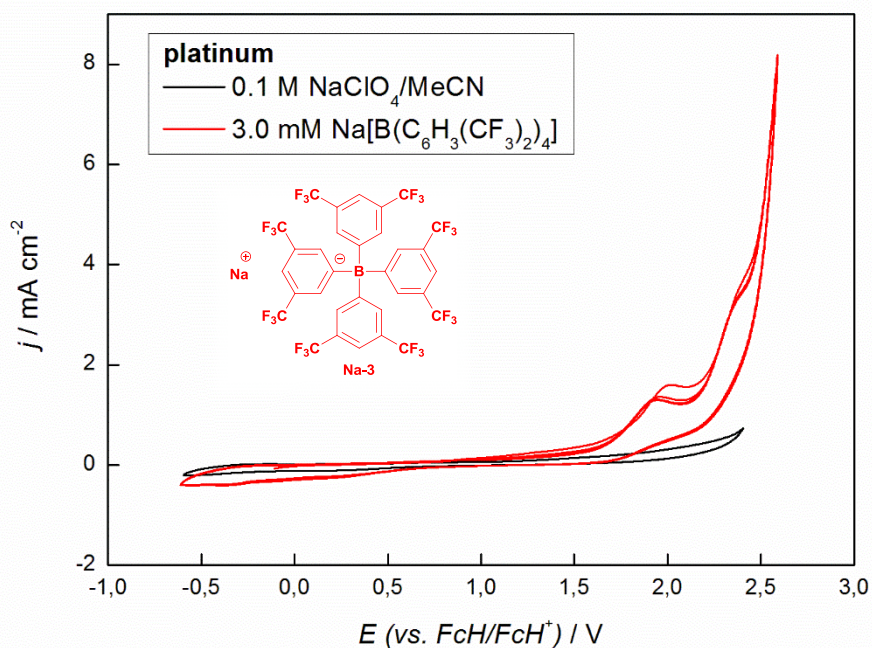


Figure S27: Cyclic voltammogram of 0.1 M NaClO₄/MeCN (black line) and 3.0 mM Na[B(C₆H₃(CF₃)₂)₄] (Na-3) (red line), working electrode: platinum, electrolyte: 0.1 M NaClO₄/MeCN, scan rate: 50 mV/s.

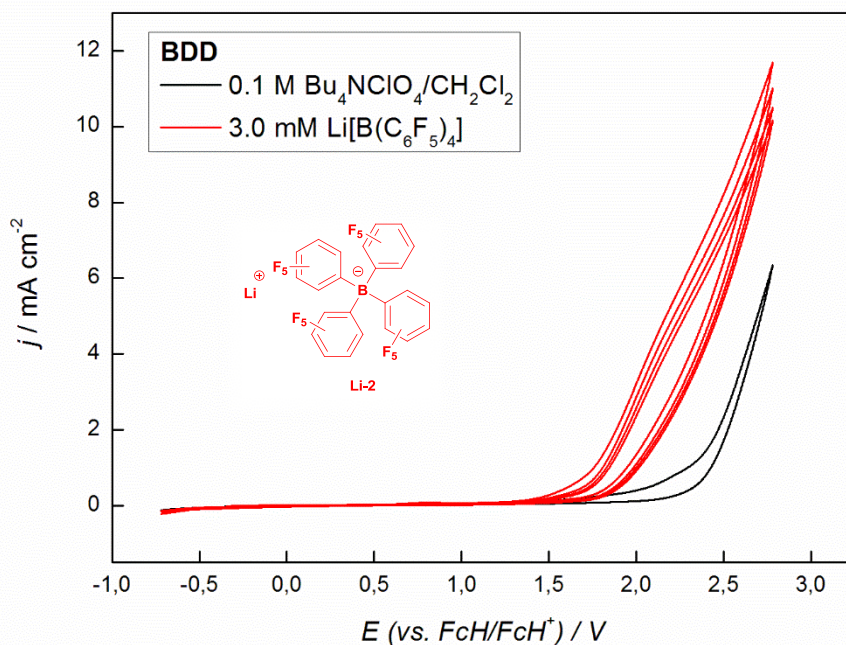


Figure S28: Cyclic voltammogram of 0.1 M Bu₄NClO₄/CH₂Cl₂ (black line) and 3.0 mM Li[B(C₆F₅)₄] (Li-2) (red line), working electrode: BDD, electrolyte: 0.1 M Bu₄NClO₄/CH₂Cl₂, scan rate: 50 mV/s.

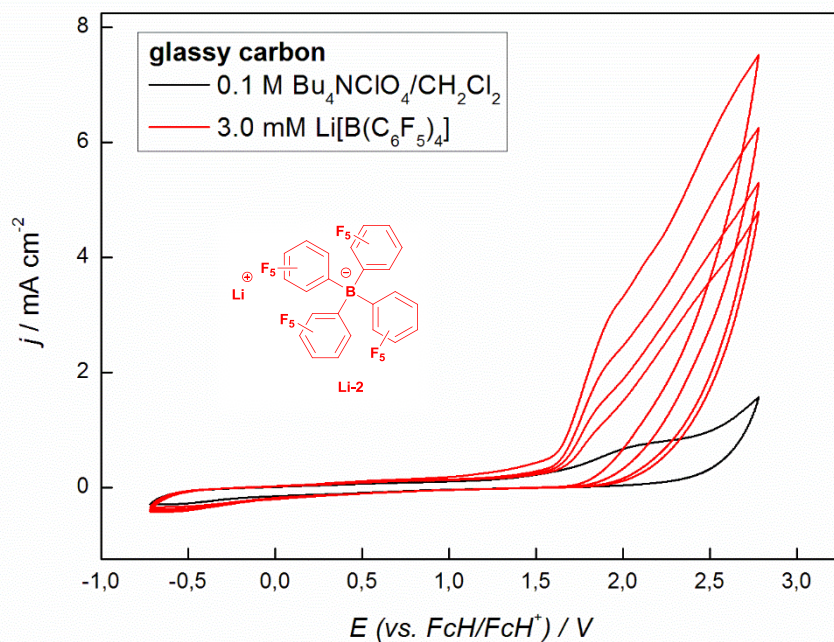


Figure S29: Cyclic voltammogram of 0.1 M $\text{Bu}_4\text{NClO}_4/\text{CH}_2\text{Cl}_2$ (black line) and 3.0 mM $\text{Li}[\text{B}(\text{C}_6\text{F}_5)_4]$ (Li-2) (red line), working electrode: glassy carbon, electrolyte: 0.1 M $\text{Bu}_4\text{NClO}_4/\text{CH}_2\text{Cl}_2$, scan rate: 50 mV/s.

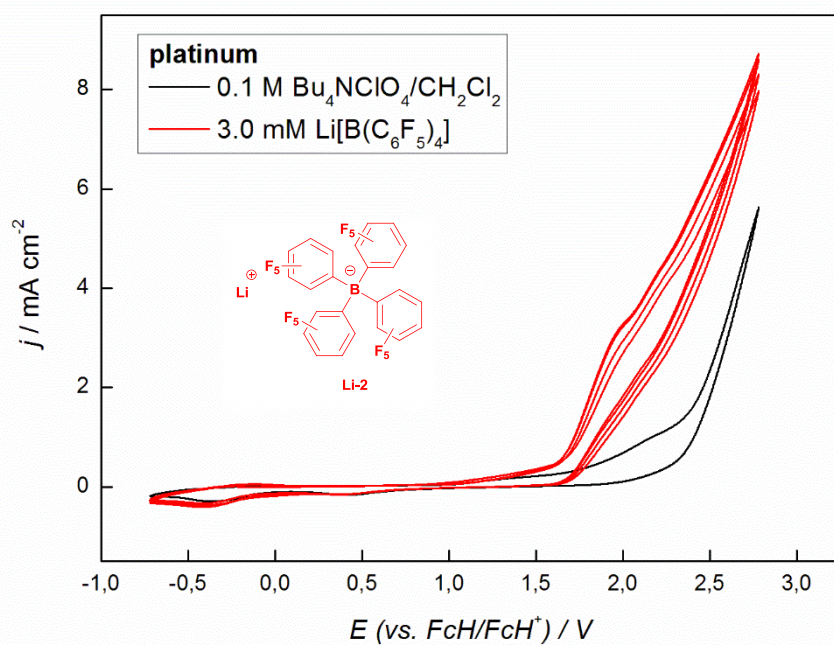


Figure S30: Cyclic voltammogram of 0.1 M $\text{Bu}_4\text{NClO}_4/\text{CH}_2\text{Cl}_2$ (black line) and 3.0 mM $\text{Li}[\text{B}(\text{C}_6\text{F}_5)_4]$ (Li-2) (red line), working electrode: platinum, electrolyte: 0.1 M $\text{Bu}_4\text{NClO}_4/\text{CH}_2\text{Cl}_2$, scan rate: 50 mV/s.

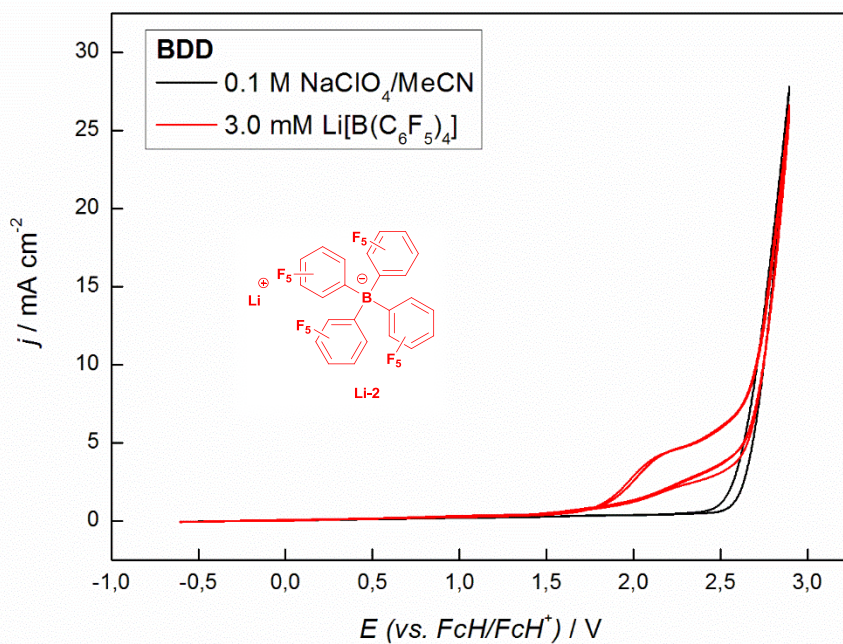


Figure S31: Cyclic voltammogram of 0.1 M NaClO₄/MeCN (black line) and 3.0 mM Li[B(C₆F₅)₄] (Li-2) (red line), working electrode: BDD, electrolyte: 0.1 M NaClO₄/MeCN, scan rate: 50 mV/s.

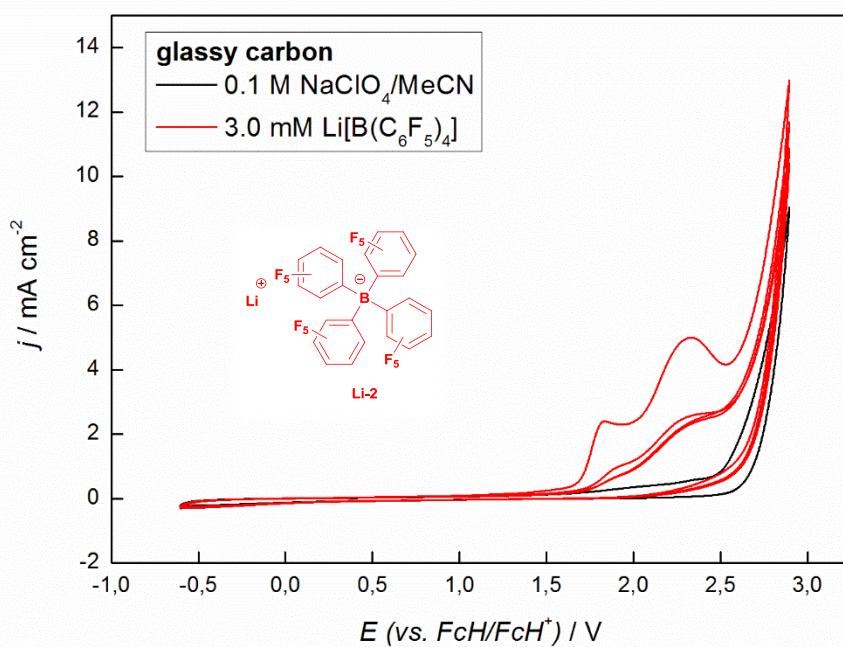


Figure S32: Cyclic voltammogram of 0.1 M NaClO₄/MeCN (black line) and 3.0 mM Li[B(C₆F₅)₄] (Li-2) (red line), working electrode: glassy carbon, electrolyte: 0.1 M NaClO₄/MeCN, scan rate: 50 mV/s.

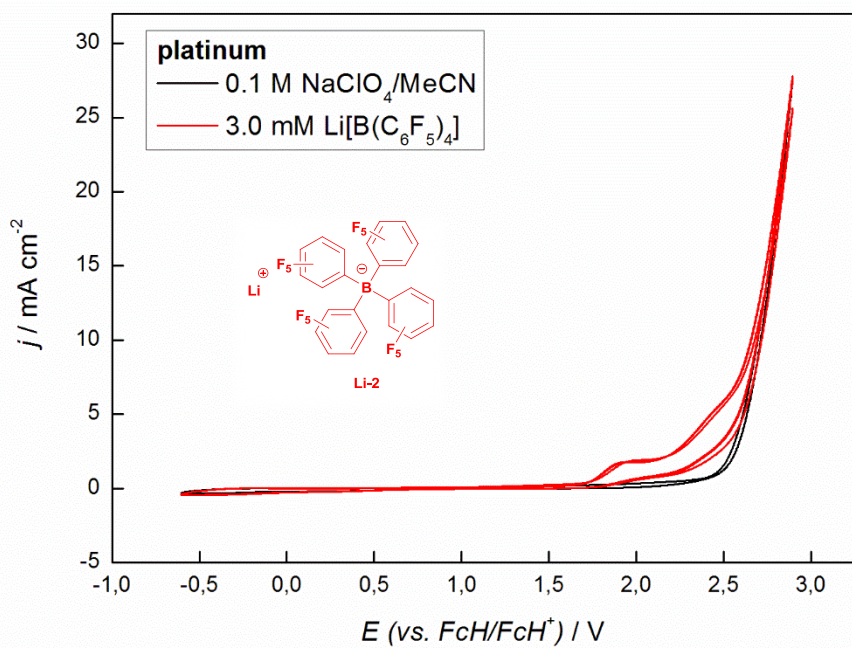
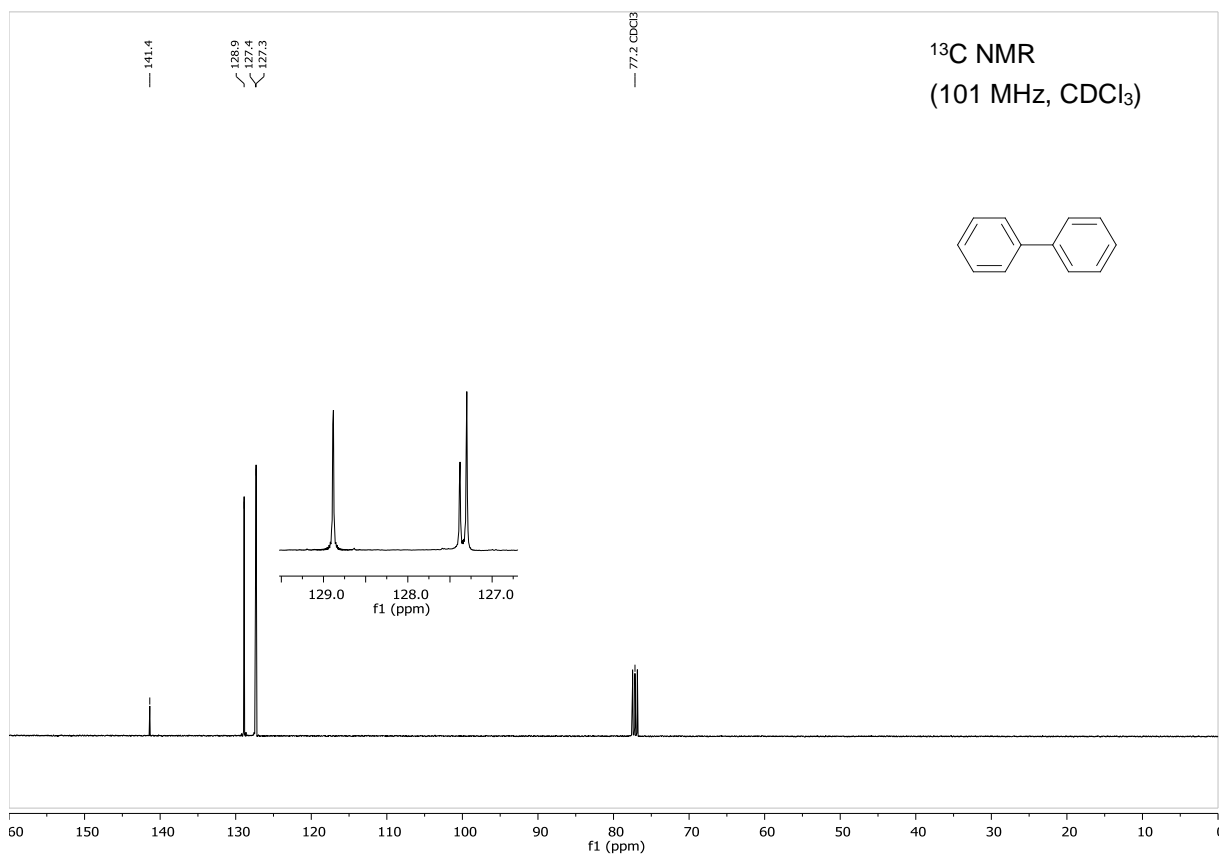
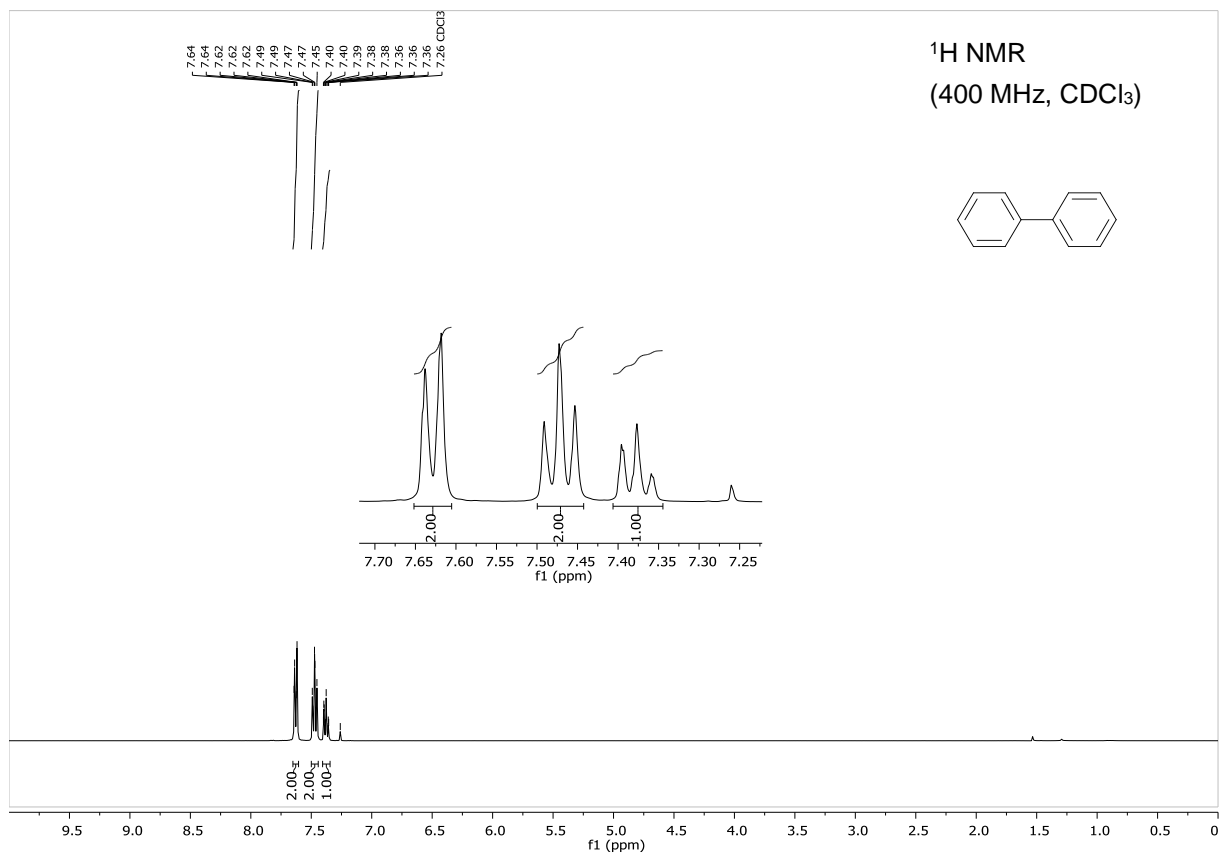


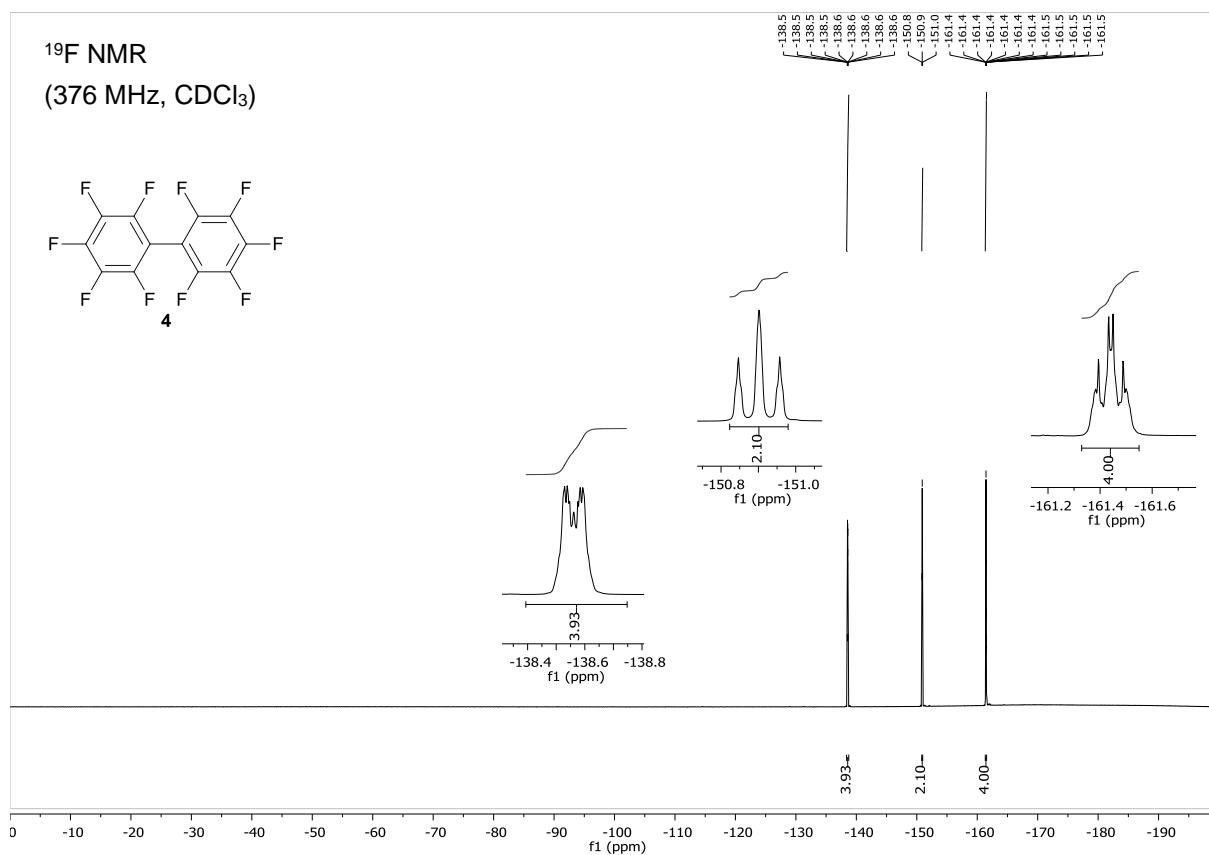
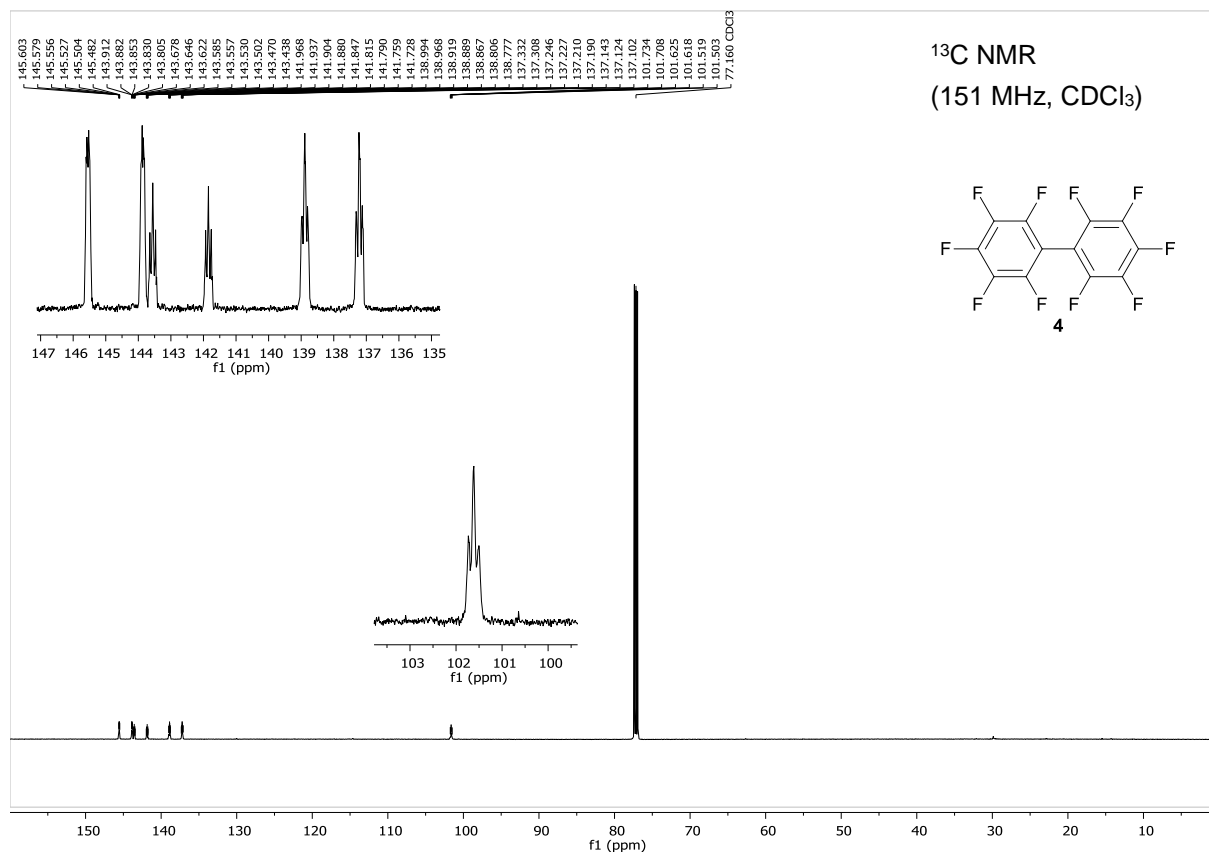
Figure S33: Cyclic voltammogram of 0.1 M NaClO₄/MeCN (black line) and 3.0 mM Li[B(C₆F₅)₄] (Li-2) (red line), working electrode: platinum, electrolyte: 0.1 M NaClO₄/MeCN, scan rate: 50 mV/s.

8. NMR Spectra

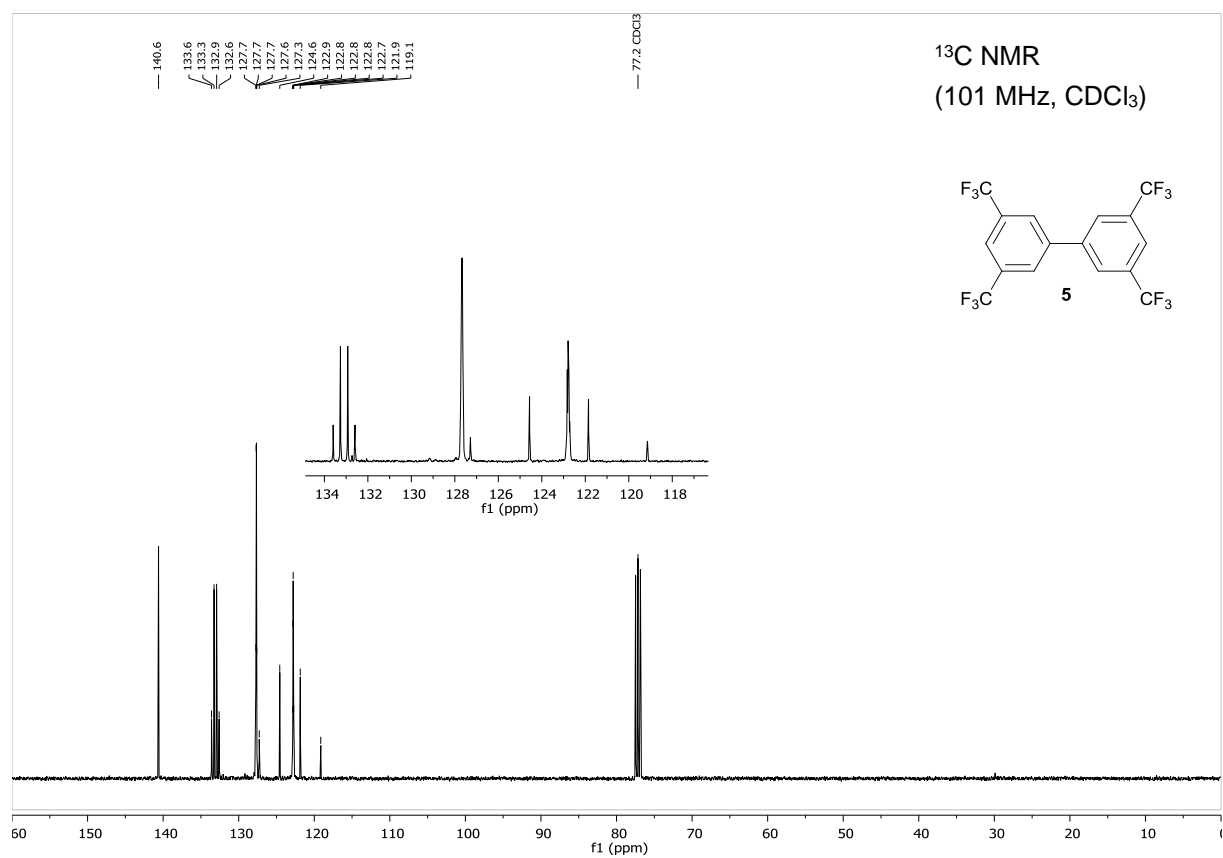
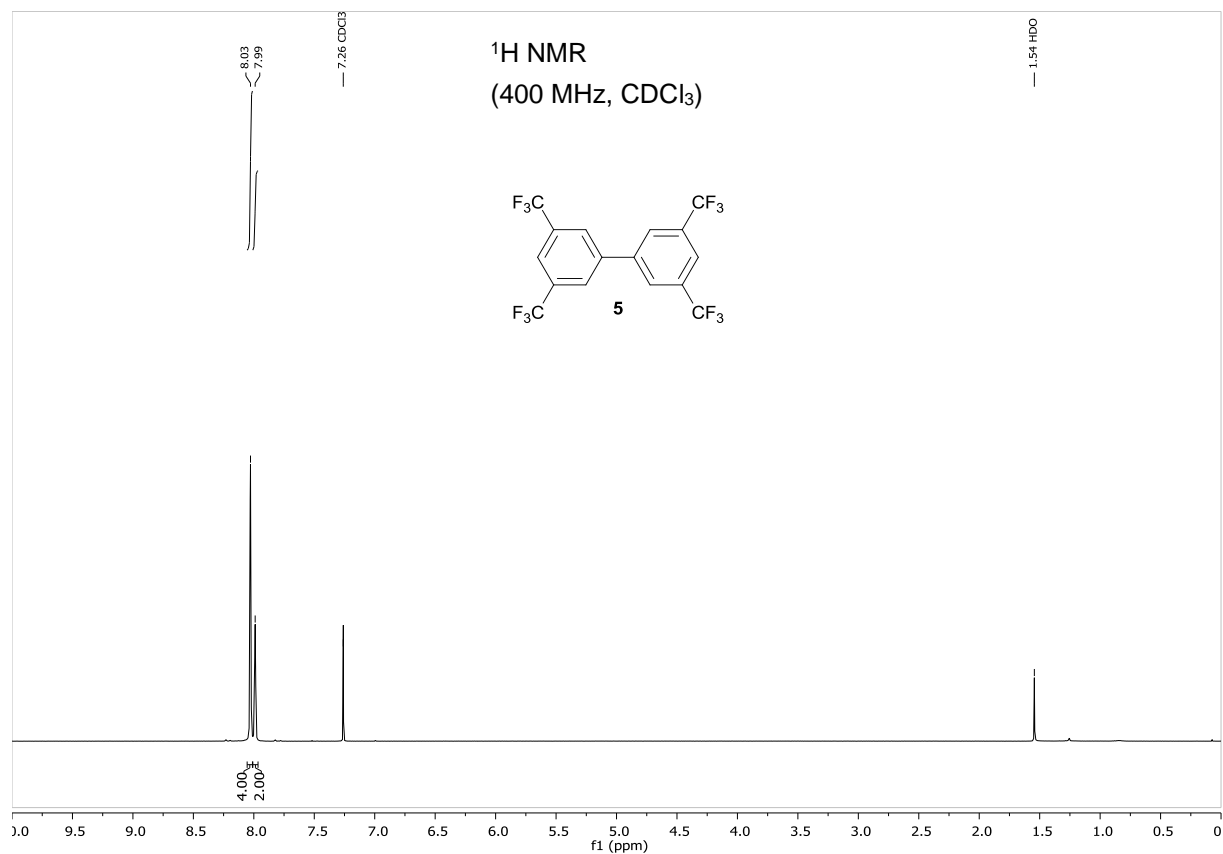
Biphenyl

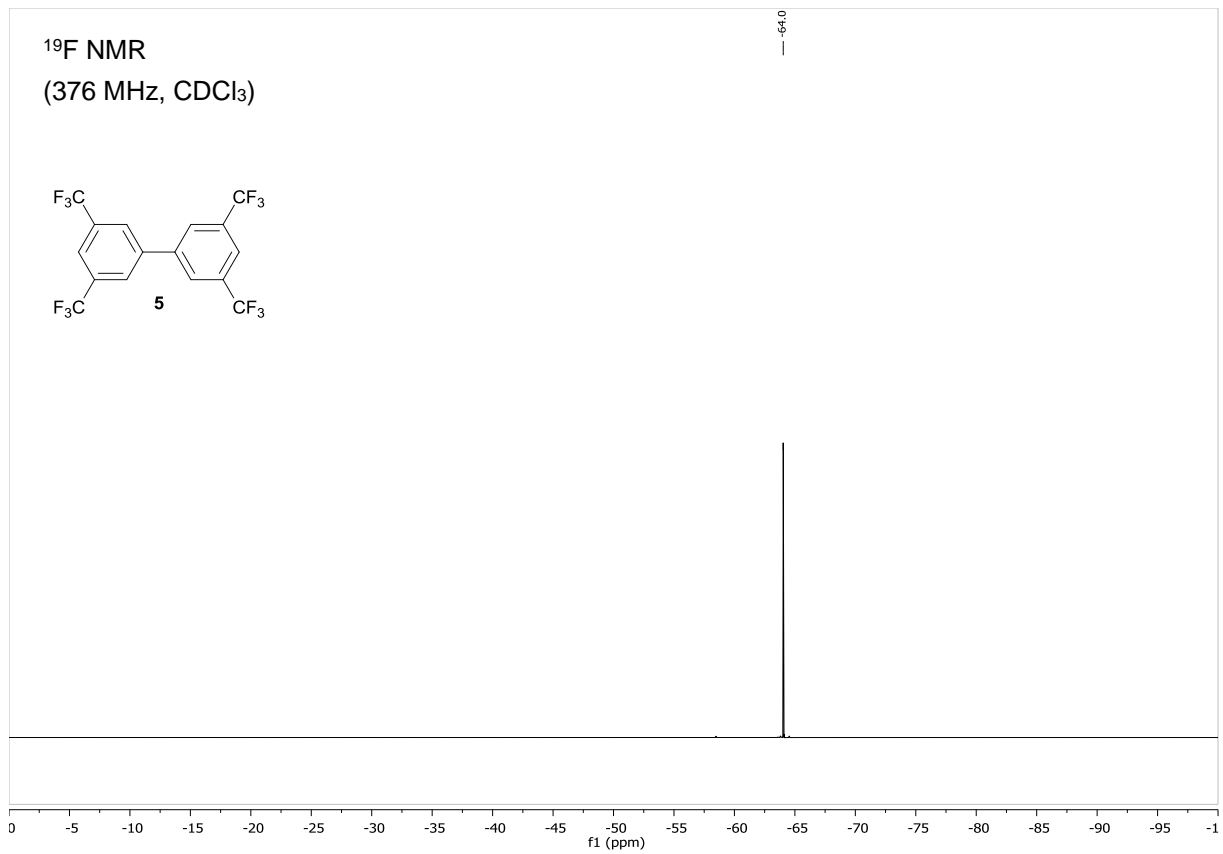


Decafluorobiphenyl (4)

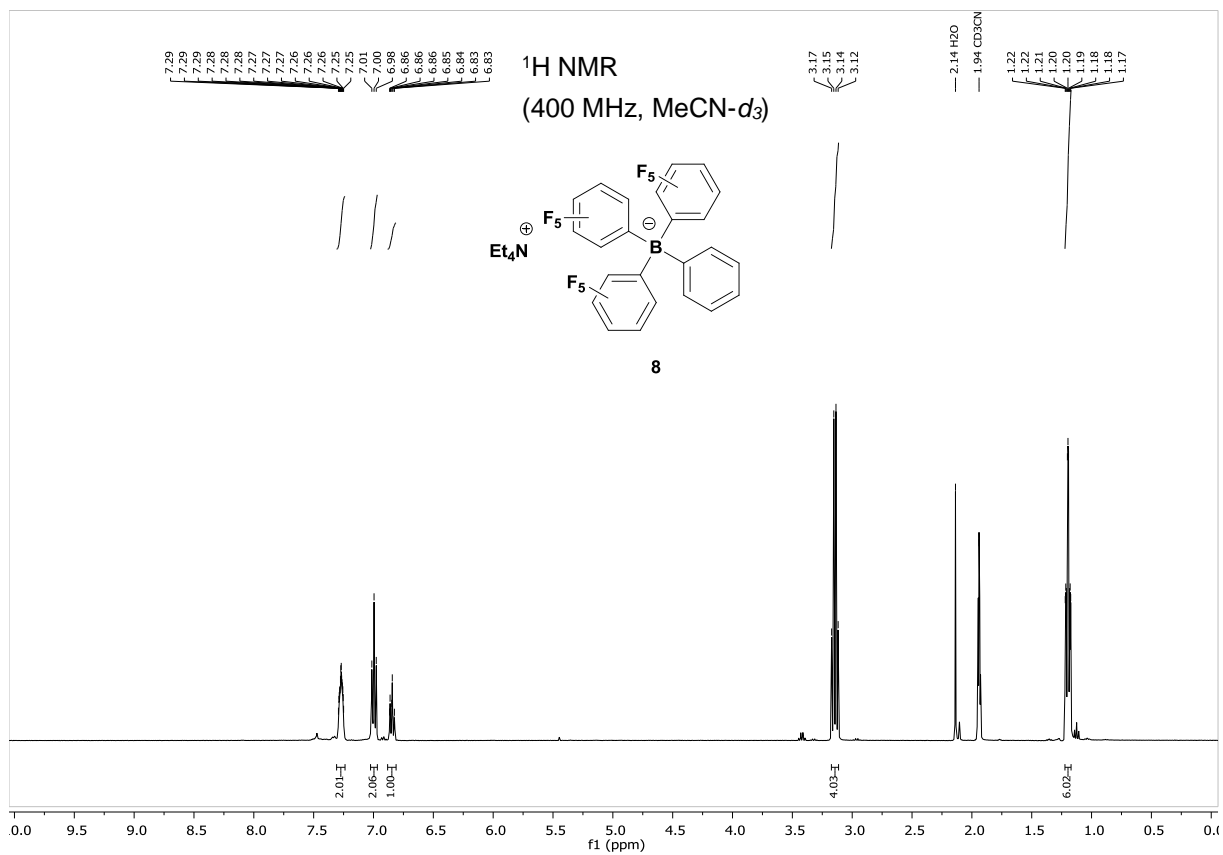


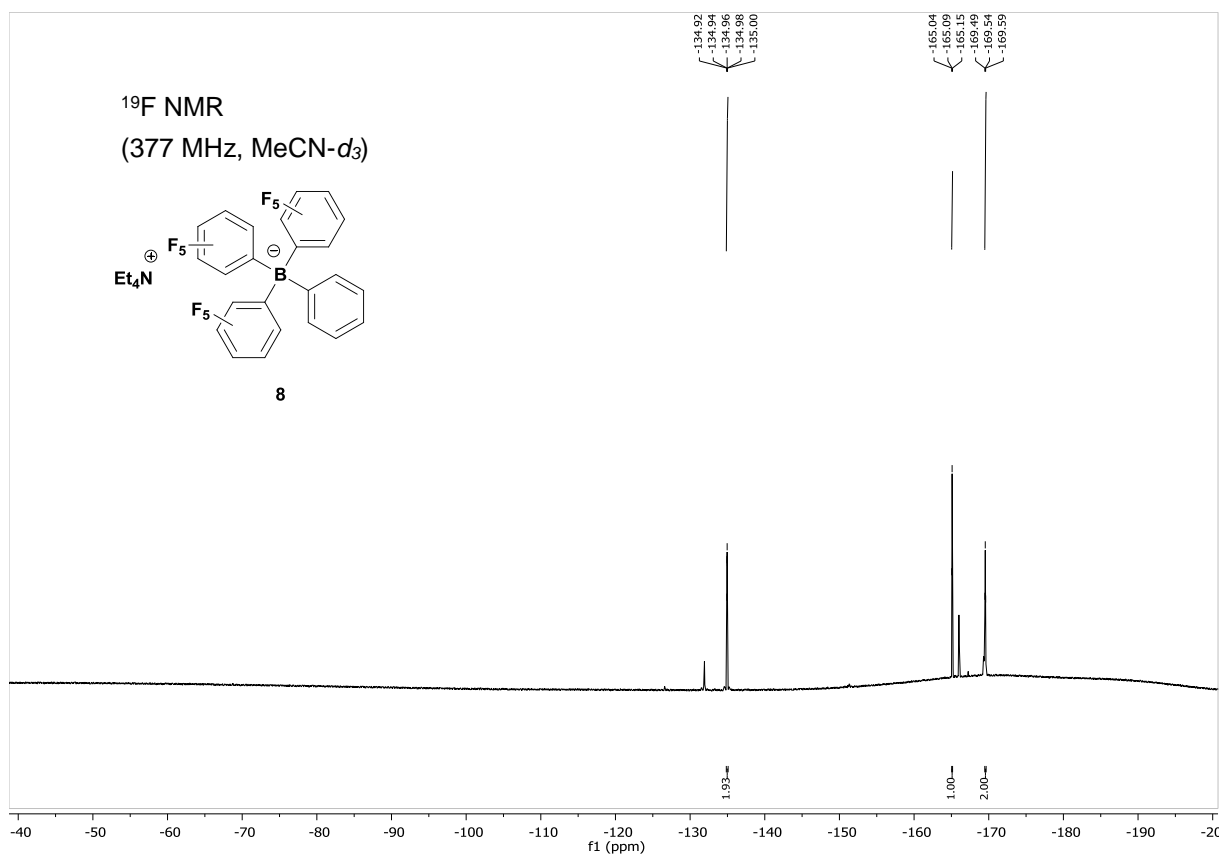
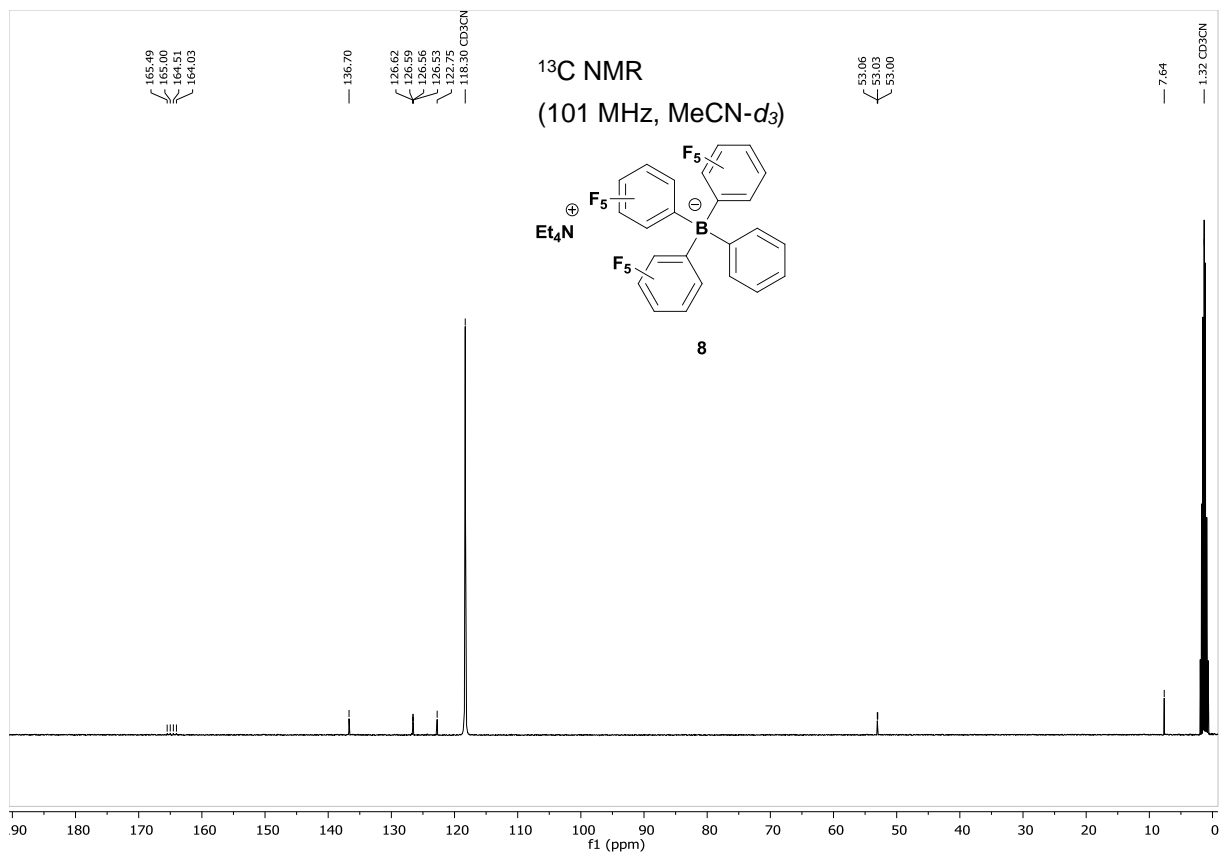
3,3',5,5'-Tetrakis(trifluoromethyl)biphenyl (5)



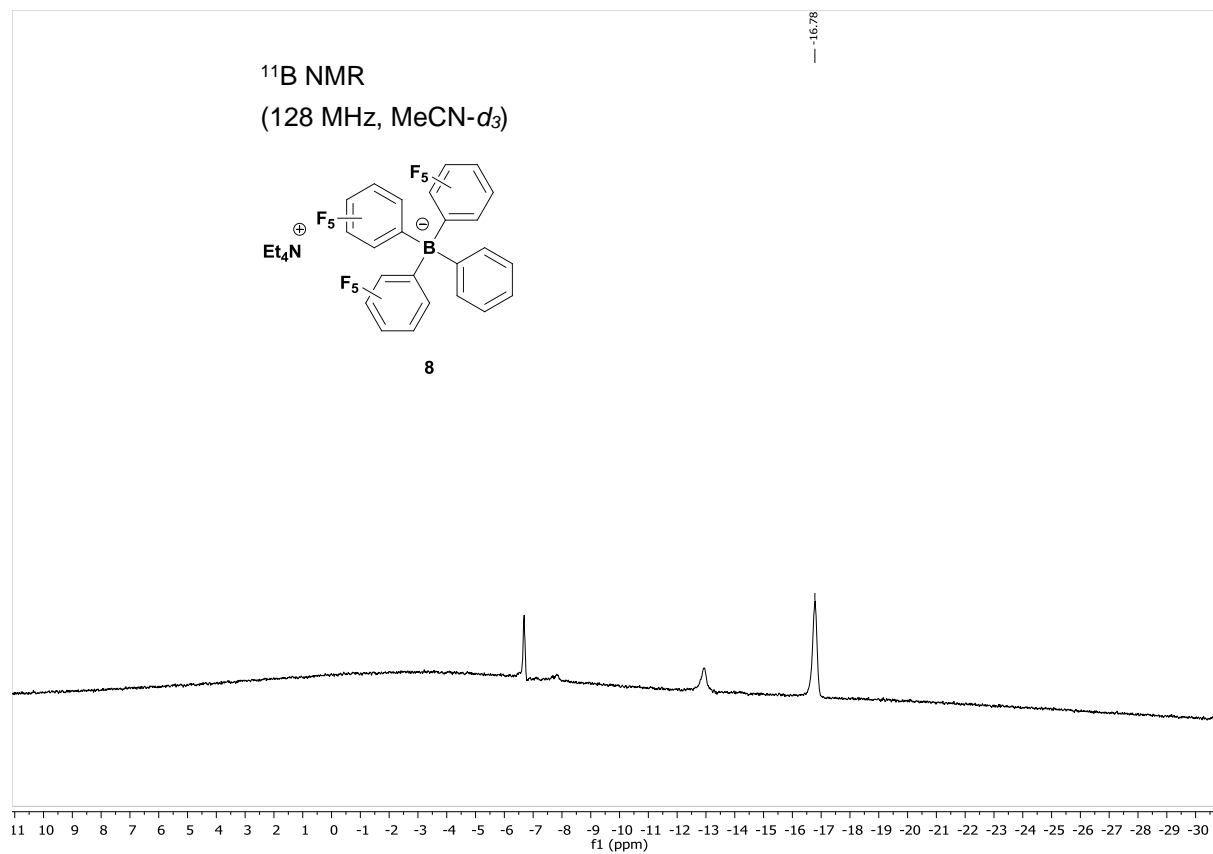
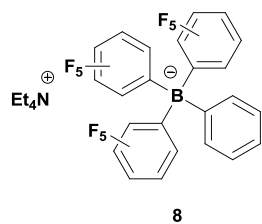


Tetraethylammonium tris(pentafluorophenyl)phenylborate (7)





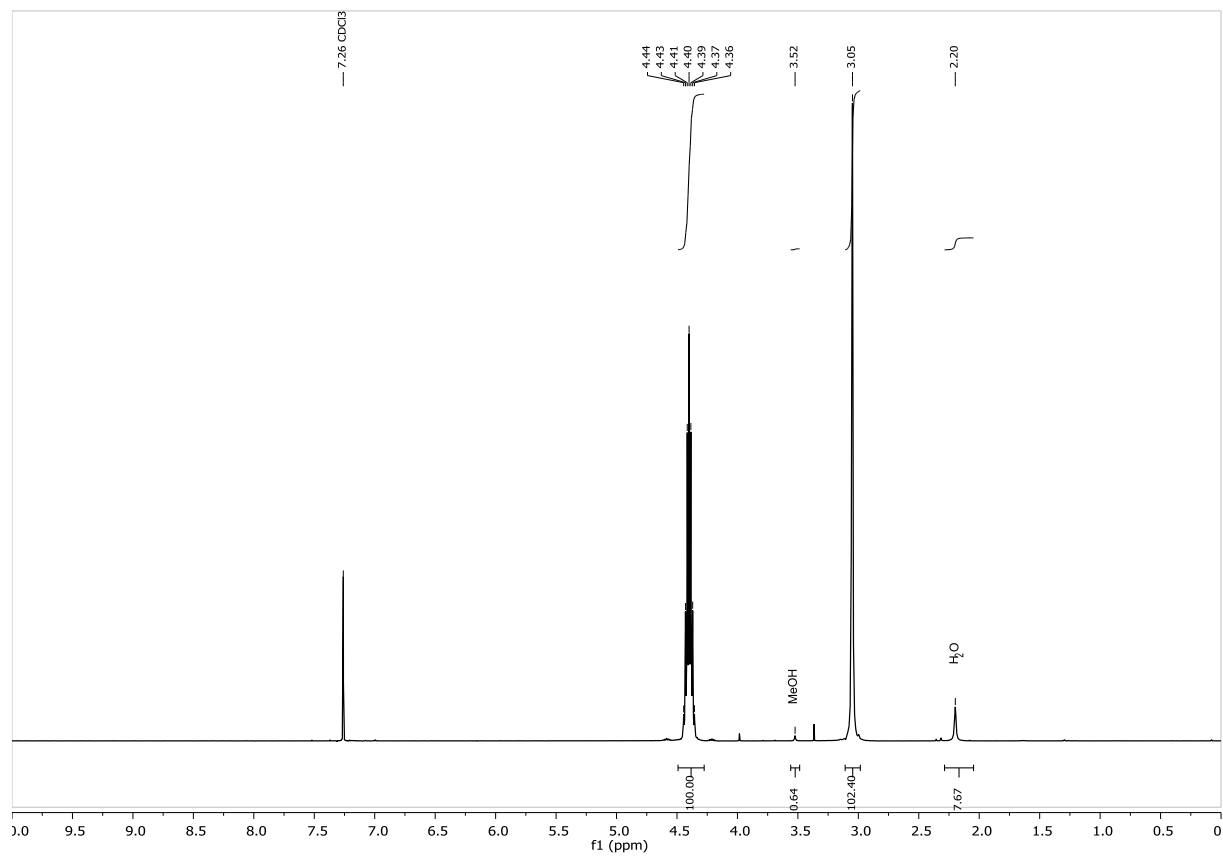
¹¹B NMR
(128 MHz, MeCN-d₃)



1,1,1,3,3,3-Hexafluoroisopropanol

Recycled HFIP: dried over P₄O₁₀ and redistilled.

¹H NMR (400 MHz, CDCl₃): δ (ppm) = 2.20 (s, 7.7 H, H₂O, CH₃OH), 3.05 (s, 102.4 H, (CF₃)₂CHOH), 3.52 (s, 0.64 H, CH₃OH), 4.40 (hept, J = 5.9 Hz, 100 H, (CF₃)₂CHOH).



9. References

- 1 V. V. Pavlishchuk and A. W. Addison, *Inorg. Chim. Acta*, 2000, **298**, 97.
- 2 C. Gütz, B. Klöckner and S. R. Waldvogel, *Org. Process Res. Dev.*, 2015, **20**, 26.
- 3 S. B. Beil, T. Müller, S. Sillart, P. Franzmann, A. Bomm, M. Holtkamp, U. Karst, W. Schade and S. R. Waldvogel, *Angew. Chem. Int. Ed.*, 2018, **57**, 2450.
- 4 X. Xu, D. Cheng and W. Pei, *J. Org. Chem.*, 2006, **71**, 6637.
- 5 a) R. Shang, Y. Fu, Y. Wang, Q. Xu, H.-Z. Yu and L. Liu, *Angew. Chem. Int. Ed.*, 2009, **48**, 9350; b) M. Lafrance, D. Shore and K. Fagnou, *Org. Lett.*, 2006, **8**, 5097.
- 6 S. D. Ross, M. Markarian and M. Schwarz, *J. Am. Chem. Soc.*, 1953, **75**, 4967.
- 7 P. K. Pal, S. Chowdhury, M. G. B. Drew and D. Datta, *New J. Chem.*, 2002, **26**, 367.